GEOPOLITICS, GEOECONOMICS, AND SOVEREIGN RISK: DIFFERENT SHOCKS, DIFFERENT CHANNELS*

VERSION OF MARCH 10TH, 2026

Alvaro Ortiz
BBVA Research & CRIW(NBER)
alvaro.ortiz@bbva.com

Tomasa Rodrigo
BBVA Research
tomasa.rodrigo@bbva.com

Pablo Saborido
BBVA Research
pablo.saborido@bbva.com

ABSTRACT

Geopolitical shocks reprice sovereign default risk directly; geoeconomic shocks bypass default risk and transmit through expected monetary policy and the global financial cycle. We document this distinction—a "scissors pattern" in which the Direct and Global Financial Cycle channels of sovereign CDS spreads move in opposite directions—using a daily panel of 42 advanced and emerging economies over 2018–2025. A Shapley–Taylor decomposition of nonlinear machine-learning predictions partitions each observation's spread into four channels: Direct, Global Financial Cycle, Uncertainty, and Local. Panel local projections under narrative identification around four dated crisis events recover the scissors at the 1% significance level for Russia–Ukraine and confirm 15 of 16 event–channel predictions. A placebo falsification shows that all four episodes exceed at least 83% of random non-event dates, with different channels exiting the envelope for each shock type. Geopolitical direct effects decay with distance from the conflict zone, while policy-uncertainty shocks activate the Uncertainty channel globally. The taxonomy implies that liquidity provision can address financial-cycle-mediated spread widening, but not the persistent component of geopolitical risk premia.

Keywords Geopolitics · Geoeconomics · Sovereign Risk · Machine Learning · Shapley–Taylor Decomposition · Transmission Channels · Global Financial Cycle · Local Projections · Text as Data

1 Introduction

Sovereign risk is a central concern for global financial stability, shaping borrowing costs, capital flows, and market resilience to shocks. Since the global financial crisis, heightened geopolitical and geoeconomic uncertainty has stimulated the development of news-based indicators of geopolitical risk (Caldara and Iacoviello, 2022), economic and trade policy uncertainty (Baker et al., 2016; Caldara et al., 2020), and political sentiment (Ahir et al., 2018; Hassan et al., 2019). These indices capture high-frequency shifts in perceptions that affect investment, asset prices, and sovereign spreads (Novta and Pugacheva, 2021; Boubaker et al., 2023). Existing work establishes that geopolitical and geoeconomic shocks widen sovereign spreads (Fernández-Villaverde et al., 2024; Boubaker et al., 2023), but whether these two shock types operate through the same transmission channels remains an open question.

This paper shows that they do not. Geopolitical shocks are associated with direct repricing of sovereign credit risk, with the global financial cycle providing a transient offset—a "scissors pattern" in which the Direct and Global Financial Cycle (GFC) channels move in opposite directions. Geoeconomic shocks largely bypass the Direct channel and are instead associated with movements in financial conditions and policy uncertainty. These channels differ in persistence—fundamental repricing endures while financial amplification mean-reverts (Bekaert et al., 2013; Bloom et al., 2018)—and in cross-sectional structure: geopolitical direct effects decay with geographic distance from the

*The authors thank, without implicating, Stephen Hansen (UCL), Daniel J. Lewis (UCL), Andreas Joseph (Bank of England), Juri Marcucci (Banca d'Italia), Santiago E. Alvarez-Blaser (Bank of Spain), Marina Diakonova (Bank of Spain), Javier Perez (Bank of Spain), Martin Saldias (Bank of Portugal) and participants in the internal seminar of Bank of Spain and BBVA research. We especially thank Buket Begun Boga, Patricia Soroa and Ismael Frutos for their contribution to build the database.

conflict zone, while policy-uncertainty shocks activate the Uncertainty channel globally and simultaneously (Pástor and Veronesi, 2012, 2013). The distinction carries direct policy implications: GFC-mediated widening is addressable through central-bank liquidity provision (Bahaj and Reis, 2022); direct sovereign repricing is not.

The paper makes three contributions. *First*, we construct a daily panel pairing sovereign CDS spreads with harmonized, local-language news-based indicators for 42 advanced and emerging economies over 2018–2025. A systematic ML horse race confirms that these indicators substantially improve out-of-sample forecasts, but primarily when nonlinear models are used—implying that the predictive content of news operates through interactions and threshold effects that linear frameworks understate.

Second, we develop a four-channel Shapley–Taylor decomposition that exactly partitions each observation's predicted spread into a Direct effect, a GFC channel, an Uncertainty channel, and a Local Macro-Political channel. Applied to four crisis episodes—the Russia–Ukraine invasion, the Hamas–Israel conflict, the 2024 U.S. presidential election, and the "Liberation Day" tariff announcement—this framework reveals the scissors pattern and a descriptive taxonomy: geopolitical episodes activate the Direct channel, whereas geoeconomic episodes largely bypass it. The cross-sectional anatomy is equally distinctive: direct geopolitical effects decay with distance from the conflict zone in a gravity-style pattern (Head and Mayer, 2014).[2] An originator penalty also emerges whereby geoeconomic-shock originators face widening spreads through the Local channel even as monetary easing compresses spreads abroad.

Third, we subject this taxonomy to a separate econometric validation using panel local projections (Jordà, 2005) under two complementary identification strategies. Full-sample innovation residuals recover qualitative sign patterns consistent with the taxonomy, but aggregate responses are often muted because the scissors mechanism causes offsetting channels to cancel out. A narrative strategy based on four exogenous dated events recovers the full transmission anatomy: the scissors pattern emerges at the 1% significance level for Russia–Ukraine, and 15 of 16 event–channel predictions are confirmed across the four episodes. A placebo falsification exercise using driver-specific decompositions confirms that all four episodes produce channel divergence exceeding at least 83% of random non-event dates, with the identity of the channels exiting the envelope differing across shock types in the direction the taxonomy predicts. Because this validation is separate from the ML estimation stage, it provides complementary evidence that the channel assignments reflect properties of transmission rather than artifacts of model fitting.

The three layers are sequentially dependent: without nonlinear models, threshold-dependent transmission is missed; without Shapley–Taylor interactions, the channels cannot be constructed; without local projections, the channel assignments lack independent validation. The paper proceeds as follows. Section 2 describes the database. Section 3 presents the ML framework, the Shapley–Taylor channel decomposition, and the local projection design. Section 4 evaluates predictive performance and Shapley-based results. Section 5 develops the four-channel taxonomy across four crisis episodes. Section 6 provides econometric validation via local projections. Section 7 concludes.

Related Literature

Our analysis connects to five literatures. On *news-based uncertainty and sentiment*, we build on indices of economic policy uncertainty, trade policy uncertainty, and geopolitical risk (Baker et al., 2016; Caldara et al., 2020; Caldara and Iacoviello, 2022) and on evidence that local-language news sources capture domestic risk perceptions more accurately than global outlets (Bondarenko et al., 2024; Alonso-Alvarez et al., 2025; Gentzkow et al., 2019).

On *geopolitics, geoeconomics, and sovereign risk*—a rapidly growing field surveyed by Mohr and Trebesch (2025)—geopolitical risk has been shown to widen spreads (Fernández-Villaverde et al., 2024; Boubaker et al., 2023) and trade tensions to amplify uncertainty (Ahn and Ludema, 2020; Aiyar et al., 2023; Fernández-Villaverde et al., 2025); we extend this work by showing that these two shock types enter through qualitatively different transmission channels. This distinction connects to the theoretical framework of Clayton et al. (2026), who model how economic interdependence creates both vulnerability and leverage in geoeconomic relationships; our four-channel decomposition provides the sovereign-risk counterpart to their structural analysis. At the firm level, Clayton et al. (2025) use large language models to extract geoeconomic pressure from earnings calls; our analysis complements theirs by tracking how these same forces transmit through sovereign credit markets at daily frequency.

On the *structure of sovereign credit risk*, Longstaff et al. (2011) decompose sovereign CDS into a default-probability component and a risk-premium component driven by global financial variables. For geopolitical shocks, this partition maps onto our Direct and GFC channels; for geoeconomic shocks, the Direct channel is small and transmission operates through the remaining three—a distinction the two-component framework leaves unresolved. Augustin et al. (2022) document that both local fundamentals and global sentiment shape spread dynamics; our decomposition extends these

[2]The regional component of the Local channel shows no distance gradient ($R^2 = 0.003$, $p = 0.72$), validating the absorption of regional indicators into the Local channel rather than a separate fifth channel. See Section 5 and Appendix Figure 13.

frameworks by adding Uncertainty and Local channels. Pástor and Veronesi (2013) predict that uncertainty and impact premia can move in opposite directions and that the originating country bears the largest premium—Section 5 evaluates both predictions.

On the *Global Financial Cycle*, work on push–pull factors (Calvo et al., 1996; Rey, 2013; Miranda-Agrippino and Rey, 2020) and on dollar funding conditions (Du et al., 2018; Bahaj and Reis, 2022; Maggiori et al., 2020) has established the role of U.S. monetary policy and global volatility. Gopinath et al. (2025) document how geopolitical alignment is reshaping trade and capital flows; we show how these forces manifest in sovereign credit markets at daily frequency through a richer informational environment that includes news-based indicators.

On *causal identification*, our three-layer design—ML discovery, Shapley–Taylor channel construction, narrative confirmation—connects to the local projection literature (Jordà, 2005; Plagborg-Møller and Wolf, 2021), to narrative identification (Romer and Romer, 2010; Antolín-Díaz and Rubio-Ramírez, 2018), and to applications combining ML with causal inference (Athey and Imbens, 2019; Chernozhukov et al., 2024; Mullainathan and Spiess, 2017; Gu et al., 2020). Our design differs from existing ML-plus-causal approaches in that the Shapley–Taylor layer creates the channel objects that the local projection layer then validates, establishing a division of labor between nonlinear discovery and linear causal inference.

2 Data and Measurement

We assemble a daily panel of sovereign credit risk and its potential drivers for 42 advanced and emerging economies over January 2018 to July 2025.[3] The dependent variable is the 5-year sovereign credit default swap (CDS) spread—the annualized premium a protection buyer pays to insure against a credit event on sovereign debt.[4] A large literature documents that sovereign spreads respond to both macroeconomic fundamentals and shifts in global investor sentiment (Longstaff et al., 2011; Pan and Singleton, 2008; Aizenman et al., 2013; Augustin et al., 2022); our channel decomposition formalizes this distinction. All variables are smoothed using a 28-day moving average to mitigate daily noise and then standardized to zero mean and unit variance within each country. We do not perform outlier treatment, as extreme events are informative signals of exceptional shifts in risk perception. The panel is unbalanced; country-specific data availability and percentile distributions are detailed in Appendix A.

Our main contribution on the measurement side is the construction of daily, country-level news-based indicators from the *Global Database of Events, Language, and Tone* (GDELT), an open-source platform that monitors broadcast, print, and online media in more than 100 languages (Leetaru and Schrodt, 2013).[5] Following Bondarenko et al. (2024) and Alonso-Alvarez et al. (2025), we construct all indicators from *local-language* media rather than foreign or global outlets, because local newspapers more accurately reflect how geopolitical risks and policy uncertainties are perceived domestically.[6]

We construct two types of news-based indicators. *Coverage-based* indicators measure uncertainty solely through the volume of relevant news. For Economic Policy Uncertainty (EPU) and Trade Policy Uncertainty (TPU), we compute the daily share of articles containing predefined uncertainty-related keywords following Baker et al. (2016), divided by total daily news volume. Complete keyword lists are provided in Appendix A. *Tone-weighted* indicators combine volume with sentiment. For Economic Sentiment (ECO), Interest Rate Sentiment (INT), Geopolitical Risk (GPR), and Political Tensions (POL), we score relevant articles using over 40 GDELT sentiment dictionaries, yielding a tone score from -10 to $+10$, and multiply it by normalized coverage. The product is inverted so that higher values consistently correspond to greater risk.[7]

[3]The sample includes Argentina, Australia, Austria, Belgium, Brazil, Canada, Chile, China, Colombia, Czech Republic, Denmark, Egypt, Finland, France, Germany, Hungary, India, Indonesia, Israel, Italy, Japan, Jordan, Malaysia, Mexico, Morocco, Netherlands, Norway, Peru, Philippines, Poland, Qatar, Russia, Saudi Arabia, Sweden, Spain, Thailand, Turkey, Ukraine, United Kingdom, United States, Uruguay, and Vietnam.

[4]The 5-year tenor is selected because it is the most liquid and widely traded segment of the CDS curve, establishing it as the standard benchmark for pricing default probability. Unlike government bond yield spreads, CDS spreads isolate default expectations from funding costs, interest rate risk, and bond-specific supply dynamics.

[5]An alternative source is the Dow Jones Factiva database, a premium archive widely used in academic research. The historical component of the Economic Policy Uncertainty index, for example, is constructed from Factiva news archives.

[6]Bondarenko et al. (2024) show that local-source measures embed heterogeneity in national perspectives and geographic proximity to conflict that global coverage smooths away. Alonso-Alvarez et al. (2025) formalize *bilateral geopolitical risk* and document that local-source shocks have significant effects on domestic financial markets, whereas Anglosphere-media indicators systematically understate local impacts.

[7]Detailed construction formulas for all indicators are provided in Appendix A. The complete set of daily and weekly indicators is publicly available at `https://bigdata.bbvaresearch.com/en/`.

Table 1 summarizes the full set of variables.[8] The explanatory variables fall into three groups: global financial conditions, domestic macroeconomic sentiment, and political–geopolitical risk.

Table 1: Variable, Sources, and Economic Interpretation

Variable	Abbr.	Type / Source	Description
Dependent variable			
Sovereign CDS spread	CDS	Market (5Y)	Annualized premium on sovereign default insurance
Global financial variables			
U.S. 2-year Treasury yield	FED	Market	Proxy for the monetary policy stance (Swanson, 2021)
CBOE Volatility Index	VIX	Market	Implied S&P 500 volatility; global risk aversion
Domestic macroeconomic sentiment (GDELT, local-language media)			
Economic Sentiment	ECO	Tone × coverage	Narrative framing of the domestic economy
Interest Rate Sentiment	INT	Tone × coverage	Expectations on monetary policy and borrowing costs
Econ. Policy Uncertainty	EPU	Coverage-based	Ambiguity regarding economic policy decisions
Trade Policy Uncertainty	TPU	Coverage-based	Uncertainty on trade rules, tariffs, and disputes
Political and geopolitical risk (GDELT, local-language media)			
Geopolitical Risk	GPR	Tone × coverage	International conflict, military disputes, terrorism
Political Tensions	POL	Tone × coverage	Domestic instability, unrest, political contestation

The use of local-language sources is not merely a data-collection choice; it reflects a substantive measurement decision. English-language indices such as the global GPR of Caldara and Iacoviello (2022)—constructed from ten Anglosphere newspapers—measure when a country attracts international media attention, not how geopolitical risk is perceived domestically. Bondarenko et al. (2024) demonstrate this distinction sharply: geopolitical risk shocks identified from local Russian-language newspapers have significant adverse effects on the Russian economy, whereas shocks from English-language sources do not. Alonso-Alvarez et al. (2025) formalize bilateral geopolitical risk and show that Anglosphere-media indicators systematically understate local financial-market impacts. Because our decomposition attributes sovereign spread movements to country-specific news indicators, the accuracy of these indicators at the country level is a first-order concern: mismeasured local risk would contaminate the Direct and Local channels and bias the transmission taxonomy.

Figure 7 (in the Appendix A.2)reveals that unconditional associations between news-based indicators and sovereign spreads are modest and heterogeneous. For GPR, the fitted slopes are positive but shallow, becoming visible only at high stress levels in EM Europe and MENA. EPU displays a clearer positive association in emerging markets, while TPU is the noisiest indicator with limited systematic patterns. The diffuse scatter clouds suggest that unconditional relationships mask important conditioning on global financial conditions and domestic sentiment—anticipating the more interpretable patterns that emerge in the SHAP-based decompositions of Section 4.

3 Econometric Framework

Our empirical framework has three steps. First, we compare a broad set of forecasting models and select the specification with the best pseudo-real-time out-of-sample performance (Section 3.1). Second, holding that specification fixed, we use Shapley–Taylor interaction values to decompose fitted forecasts into four economically interpretable transmission channels (Section 3.2). Third, we assess whether this taxonomy receives independent support in panel local projections under two identification strategies (Section 3.3).

3.1 Forecasting Model Comparison

We model sovereign risk as a potentially nonlinear function of market and news-based predictors. For country i on date t, model class m delivers the one-step-ahead forecast

$$y_{i,t+1} = f_m(\boldsymbol{X}_{i,t}, \boldsymbol{\lambda}_i) + \varepsilon_{i,t+1}, \tag{1}$$

where $y_{i,t+1}$ is the standardized sovereign CDS spread, $\boldsymbol{X}_{i,t}$ is the information set available at date t, and $\boldsymbol{\lambda}_i$ denotes country fixed effects. We compare fifteen model classes spanning linear regression, penalized linear models (Hoerl and

[8] Our focus on high-frequency news-based indicators complements existing work emphasizing structural determinants of external debt dynamics.

Kennard, 1970; Tibshirani, 1996; Zou and Hastie, 2005), tree-based ensembles (Breiman, 2001; Friedman, 2001), and neural networks (LeCun et al., 2015).

Forecasts are generated recursively in pseudo-real time using an expanding estimation window and a 28-day exclusion buffer around each train–test split to prevent leakage from overlapping moving-average windows.[9] Model selection is based exclusively on pooled out-of-sample MAE and RMSE. Once the preferred architecture and hyperparameters are selected, they are held fixed. We then re-estimate that specification on the full estimation sample and use the fitted model only for the interpretability exercise in Section 3.2. This separation ensures that model selection is not influenced by the decomposition stage.

To quantify the incremental predictive value of news-based indicators, we compare two predictor sets. The *Markets-Only* benchmark contains the VIX and the U.S. two-year Treasury yield, providing a parsimonious baseline centered on the Global Financial Cycle (Calvo et al., 1996; Rey, 2013; Miranda-Agrippino and Rey, 2020). The augmented specification adds six news-based indicators: geopolitical risk (GPR), economic policy uncertainty (EPU), trade policy uncertainty (TPU), and three domestic macro-political indicators (ECO, INT, POL). For each model class, the change in out-of-sample loss between the two predictor sets measures the marginal predictive contribution of news and reveals which forecasting technologies are most effective in exploiting it. Section 4 reports results; the core finding is that news variables improve all model classes, but gains are substantially larger for nonlinear methods (15–19%) than for linear specifications (5–9%), implying that the predictive content of news operates through interactions and threshold effects (Varian, 2014; Gu et al., 2020).[10]

3.2 Shapley-Based Channel Decomposition

After selecting the preferred forecasting specification, we freeze its architecture and use it solely for interpretability—the Shapley analysis attributes predictions, not causal effects. Although the target variable is $y_{i,t+1}$, the decomposition is evaluated on the predictor vector observed at date t. Accordingly, the object being decomposed is the fitted forecast $\hat{y}_{i,t+1|t} = f^{\star}(\boldsymbol{X}_{i,t})$, and all channel contributions are indexed by the information date t.

Economic logic of the four channels. We partition the predictors into four blocks based on their economic role: a *global financial cycle* block $\mathcal{G} = \{\text{VIX}, \text{US2Y}\}$ containing the two variables common to all 42 countries; an *economic and trade uncertainty* block $\mathcal{U} = \{\text{EPU}, \text{TPU}\}$; a *domestic macro-political* block $\mathcal{L} = \{\text{ECO}, \text{INT}, \text{POL}\}$; and a *regional structure* block $\mathcal{R} = \{\text{REG}\}$, where REG denotes regional group indicators that encode geographic, institutional, and income-group heterogeneity.[11] We absorb $\mathcal{R}$ into the Local channel rather than introducing a fifth channel because regional structure operates as a conditioning factor that modulates the domestic amplification of external shocks, not as an independent transmission mechanism.[12]

Substantively, the Local channel variables—economic sentiment, interest-rate expectations, political tensions, and regional structure—provide daily-frequency proxies for the core determinants of sovereign creditworthiness identified by debt sustainability analysis: GDP growth prospects (ECO), the interest rate–growth differential (INT), institutional quality and policy credibility (POL), and structural vulnerability characteristics (REG). The channel thus captures domestic amplification through fundamentals, not sentiment divorced from macroeconomic conditions.

These blocks motivate four channels, each isolating a distinct transmission mechanism. The *Direct channel* measures a driver's own contribution orthogonal to all other predictors—for GPR, the pure sovereign risk premium from conflict exposure; for EPU, fiscal credibility and regulatory ambiguity; for TPU, the real trade-exposure channel. The *GFC channel* aggregates interactions with VIX and US2Y, capturing transmission through the global risk-taking and monetary environment (Rey, 2013; Miranda-Agrippino and Rey, 2020). The *Uncertainty channel* captures cross-reinforcement among policy-uncertainty measures—how conflict cascades into trade uncertainty through sanctions, or how tariff uncertainty compounds broader policy unpredictability (Bloom, 2009; Baker et al., 2016; Caldara et al., 2020). The *Local channel* collects interactions with domestic sentiment, political tensions, and regional structure, capturing the degree to which local vulnerabilities amplify or absorb external shocks. This channel structure resonates with the decomposition of sovereign spreads into default-probability and risk-premium components (Bauer et al., 2023): the

[9] Hyperparameters are selected by cross-validation within the training sample and held fixed during out-of-sample evaluation. The evaluation period runs from February 2021 to July 2025, so all four crisis episodes are assessed out of sample.

[10] The preferred specification is the Multilayer Random Forest (Two Stages), which combines near-frontier predictive performance with a substantive architectural advantage: the first stage separates advanced-economy from emerging-market panels, and the second refines predictions with region-specific dynamics

[11] Regional indicators enter the forecasting model as categorical features and generate Shapley interactions with all other predictors.

[12] Figure 4 supports this design choice: under the log-distance specification of equation (7), the Direct channel decays with distance to the conflict epicenter ($R^2 = 0.35$ for Russia–Ukraine, $p < 0.001$; $R^2 = 0.22$ for Hamas–Israel, $p < 0.01$), while the regional component of the Local channel shows no systematic relationship with distance ($R^2 = 0.003$, $p = 0.72$; Appendix Figure 13).

Direct channel isolates repricing of the sovereign's own default intensity, while the GFC channel captures risk-premium variation linked to the global financial cycle.

Formal decomposition. For each observation we compute pairwise Shapley–Taylor interaction values (Shapley, 1953; Lundberg and Lee, 2017). These attributions satisfy local accuracy, so they decompose the fitted forecast as

$$\hat{y}_{i,t+1|t} \;=\; \varphi_0 \;+\; \sum_{j=1}^{M} \varphi_{jj,i,t} \;+\; \sum_{j<k} \varphi_{jk,i,t}\,, \tag{2}$$

where φ_0 is the baseline prediction, $\varphi_{jj,i,t}$ the main effect of predictor j, and $\varphi_{jk,i,t}$ the pairwise interaction between predictors j and k.[13] The pairwise structure is essential for the channel decomposition that follows. Standard first-order Shapley values assign a single aggregate attribution to each predictor, conflating a variable's own contribution with its interactions with other predictors. The Shapley–Taylor extension separates the main effect φ_{jj} from each pairwise interaction φ_{jk}, which is what allows us to distinguish a driver's *direct* effect on sovereign risk from its *indirect* transmission through the global financial cycle, uncertainty, or domestic conditions. Without this second-order decomposition, the four-channel partition would not be identified. For any driver Z, we partition its total contribution into the four channels:

$$\underbrace{\varphi_{i,t}^{Z,\mathrm{tot}}}_{\text{total}} \;=\; \underbrace{\varphi_{ZZ,i,t}}_{\varphi_{i,t}^{Z,\mathrm{dir}}} \;+\; \underbrace{\sum_{k\,\in\,\mathcal{G}} \varphi_{Zk,i,t}}_{\varphi_{i,t}^{Z,\mathrm{GFC}}} \;+\; \underbrace{\sum_{\substack{k\,\in\,\mathcal{U}\\ k\,\neq\,Z}} \varphi_{Zk,i,t}}_{\varphi_{i,t}^{Z,\mathrm{UNC}}} \;+\; \underbrace{\sum_{\substack{k\,\in\,\mathcal{L}\,\cup\,\mathcal{R}\\ k\,\neq\,Z}} \varphi_{Zk,i,t}}_{\varphi_{i,t}^{Z,\mathrm{LOC}}} \tag{3}$$

By construction, these four terms sum to $\varphi_{i,t}^{Z,\mathrm{tot}}$ for every observation.[14] Section 5 uses these channel series to characterize how the transmission of different shock types varies over time, across countries, and across the cross-sectional distribution of sovereign risk.

3.3 Econometric Validation: Local Projections with Identified Shocks

The Shapley decomposition yields constructed channel series, but it does not by itself establish that these series capture economically meaningful transmission mechanisms. To assess whether the proposed taxonomy receives independent support, we estimate panel local projections under two identification strategies. Section 6 reports the results.

3.3.1 Panel Local Projection Specification

For each horizon $h = 0, 1, \ldots, 90$ days, we estimate:

$$\Delta_h\, Y_{i,t+h}^{ch} \;=\; \alpha_i^h \;+\; \beta^h\, S_{i,t} \;+\; \sum_{p=1}^{5} \gamma_p^h\, Y_{i,t-p}^{ch} \;+\; \delta^{h\prime}\, \mathbf{X}_{i,t} \;+\; u_{i,t+h}^h\,, \tag{4}$$

where $\Delta_h Y_{i,t+h}^{ch} \equiv Y_{i,t+h}^{ch} - Y_{i,t-1}^{ch}$ is the cumulative change in the outcome; Y^{ch} denotes either the raw standardized CDS spread or one of the four channel series $\{\varphi^{\mathrm{dir}}, \varphi^{\mathrm{GFC}}, \varphi^{\mathrm{UNC}}, \varphi^{\mathrm{LOC}}\}$; α_i^h are country fixed effects; $\mathbf{X}_{i,t}$ collects contemporaneous controls; and $S_{i,t}$ is the identified shock. This generic notation accommodates both identification strategies: under Strategy I, $S_{i,t}$ is country-specific; under Strategy II, it is common across countries for a given event date. Standard errors use the Driscoll and Kraay (1998) estimator, robust to heteroskedasticity, serial correlation up to $h+1$ lags, and cross-sectional dependence. We report 68% and 90% confidence bands throughout. The estimation covers 75,650 country–day observations.

3.3.2 Strategy I: Full-Sample Innovation Identification

We identify shocks as innovations from country-specific AR(5) processes:

$$Z_{i,t} \;=\; \mu_i + \sum_{p=1}^{5} \rho_{i,p}\, Z_{i,t-p} + \varepsilon_{i,t}^{Z}\,. \tag{5}$$

[13] Shapley values are the unique attribution satisfying local accuracy (attributions sum to the prediction) and consistency (if a feature's marginal impact increases, its attribution cannot decrease). In practice we compute pairwise interaction values using TreeSHAP. The algorithm produces a negligible numerical residual $\eta_{i,t}$ with median magnitude below $10^{-4}\sigma$; we treat the decomposition as exact throughout.

[14] When $Z \in \mathcal{U}$, the Uncertainty channel contains only the single cross-interaction between EPU and TPU. When $Z \in \mathcal{L}$, the Local channel excludes Z's own main effect, which enters the Direct channel. Regional indicators in $\mathcal{R}$ contribute to the Local channel for all drivers Z.

The standardized residual $S^Z_{i,t} = \hat{\varepsilon}^Z_{i,t} \,/\, \hat{\sigma}_{\varepsilon,i}$ serves as the shock in equation (4).[15] This strategy estimates the average marginal response to a one-standard-deviation country-level innovation, pooling across the entire sample. Its strength is broad coverage. Its limitation is that it averages over routine and crisis periods alike, which attenuates episode-specific transmission patterns—an attenuation that the scissors mechanism makes especially severe, since the offsetting Direct and GFC channels tend to cancel in aggregate.

3.3.3 Strategy II: Narrative Identification

We construct event dummies equal to one in a ± 3-day window around each of four dated events:

$$D^e_t \;=\; \mathbb{1}\big(|t - t_e| \le 3\big), \qquad e \in \{E1, E2, E3, E4\}\,, \tag{6}$$

where t_{E1} = 24 February 2022 (Russia–Ukraine invasion), t_{E2} = 7 October 2023 (Hamas–Israel attack), t_{E3} = 5 November 2024 (U.S. presidential election), and t_{E4} = 2 April 2025 ("Liberation Day" tariff announcement). A separate local projection is estimated for each event, with $S_{i,t} = D^e_t$. Each event is paired with its primary news indicator: GPR for $E1$ and $E2$, EPU for $E3$, TPU for $E4$.

The narrative approach offers two advantages. First, event timing is plausibly exogenous to day-to-day sovereign CDS movements. Second, the taxonomy generates event-specific predictions—geopolitical events should primarily activate the Direct channel, whereas geoeconomic events should largely bypass it—that the narrative local projections evaluate directly.

4 The Layered Structure of Sovereign Risk

This section establishes three facts that motivate the transmission analysis. First, news-based indicators add material predictive content beyond global financial variables, but primarily through nonlinear models. Second, in the selected specification, the largest average contributions come from global financial conditions, while domestic sentiment differentiates countries within that common environment. Third, geopolitical and policy-uncertainty indicators matter primarily through nonlinear interactions rather than through large average main effects. Together, these results motivate the four-channel decomposition developed in Section 5.

4.1 Model Selection

All predictors and the dependent variable are constructed as 28-day moving averages, so adjacent observations mechanically share underlying daily information. To avoid leakage, we evaluate all model classes in a recursive pseudo-real-time design with a 28-day exclusion buffer around each forecast origin. This buffer ensures that no training observation overlaps with the test target, so any improvement from adding news-based indicators can be interpreted conservatively as genuine incremental predictive content.[16] Table 2 reports out-of-sample forecast accuracy under the Markets-Only and Markets+News information sets. Three findings stand out. Flexible nonlinear methods outperform linear specifications, with Extremely Randomized Trees achieving the lowest errors (MAE = 0.60). News variables improve every model class, but the gains are substantially larger for nonlinear methods (15–19% RMSE reduction) than for linear specifications (5–9%), indicating that much of the predictive content of news enters through interactions and threshold effects that linear frameworks understate (Varian, 2014; Gu et al., 2020). The magnitude of improvement rises monotonically with model flexibility (Mullainathan and Spiess, 2017; Athey and Imbens, 2019).

Although Extremely Randomized Trees delivers the lowest raw forecast loss, the remainder of the paper uses the Multilayer Random Forest (Two Stages) as the baseline for interpretation. Its performance remains close to the frontier, while its architecture preserves the advanced-economy/emerging-market split and region-specific structure that are central to the subsequent decomposition.[17]

4.2 Sovereign Risk Drivers

Figure 1 summarizes the fitted model's feature importance using mean absolute Shapley values at the global, regional, and country levels.

[15] Qualitatively we obtain similar results under panel AR(5) specifications with country fixed effects or from simple first differences $\Delta Z_{i,t}$. See Appendix F.

[16] A simple AR(1) benchmark performs worse than the Markets-Only specification, confirming that the latter provides a stricter baseline.

[17] The Multilayer Random Forest extends the standard Random Forest by stacking two sequential ensemble layers (Breiman, 2001). The first layer is trained separately on advanced- and emerging-economy panels; the second combines intermediate predictions with the full set of covariates.

Table 2: **News Indicators Improve Nonlinear Forecasts of Sovereign Risk**

Machine Learning Model	Benchmark Market Only		News Extended Market + News		Difference (News Extended vs Benchmark) RMSE		MAE	
	RMSE	MAE	RMSE	MAE	Diff	% Var	Diff	% Var
Linear Regression	1.09	0.92	1.03	0.86	-0.06	-5.7%	-0.06	-6.4%
Lasso	1.03	0.87	0.95	0.80	-0.08	-8.0%	-0.08	-8.7%
Ridge	1.09	0.92	1.02	0.85	-0.07	-6.4%	-0.07	-7.2%
Elastic Net	1.04	0.88	0.95	0.79	-0.09	-8.8%	-0.08	-9.5%
Quantile Linear Regression	0.93	0.77	0.90	0.74	-0.03	-3.7%	-0.03	-4.5%
Principal Components (PCR)	1.09	0.92	0.99	0.82	-0.09	-8.6%	-0.09	-10.3%
Factor Models (FAR)	0.92	0.75	0.88	0.72	-0.04	-4.4%	-0.03	-3.6%
Gradient Boosting	1.00	0.81	0.85	0.67	-0.14	-14.2%	-0.14	-17.9%
Bagging	1.03	0.83	0.84	0.67	-0.19	-18.3%	-0.17	-20.1%
Random Forest	0.99	0.75	0.82	0.65	-0.17	-17.1%	-0.11	-14.3%
Extremely Randomized Trees	0.98	0.74	0.80	0.60	-0.18	-18.5%	-0.14	-19.0%
Multilayer Random Forest (1S)	0.97	0.75	0.84	0.62	-0.13	-13.6%	-0.13	-17.2%
Multilayer Random Forest (2S)	1.01	0.77	0.85	0.65	-0.16	-15.9%	-0.12	-15.5%
Shallow CNN	1.05	0.84	0.97	0.77	-0.09	-8.3%	-0.07	-8.8%
Deep CNN	1.04	0.77	0.89	0.66	-0.15	-14.1%	-0.11	-14.3%

Notes: Out-of-sample RMSE and MAE for one-day-ahead forecasts of standardized sovereign CDS spreads under two information sets: Markets-Only (VIX and U.S. two-year Treasury yield) and Markets+News (augmented with GPR, EPU, TPU, ECO, INT, POL). All variables are 28-day moving averages. Models are estimated recursively with a 28-day exclusion buffer. "Diff" denotes the change relative to the Markets-Only benchmark; negative values indicate lower forecast loss.

The Shapley ranking points to a layered structure. The first layer is global. The U.S. two-year yield and the VIX are the largest contributors in almost every region and for nearly every country, with mean absolute Shapley values exceeding those of any other variable— consistent with the view that sovereign spreads are anchored by common financial conditions (Rey, 2013; Miranda-Agrippino and Rey, 2020), with the VIX corroborating its role as a barometer of global risk aversion whose spikes precede capital-flow reversals and spread widening (Gelos et al., 2011).

Figure 1: **Global Financial Conditions Dominate Sovereign Risk: Shapley Feature Importance**

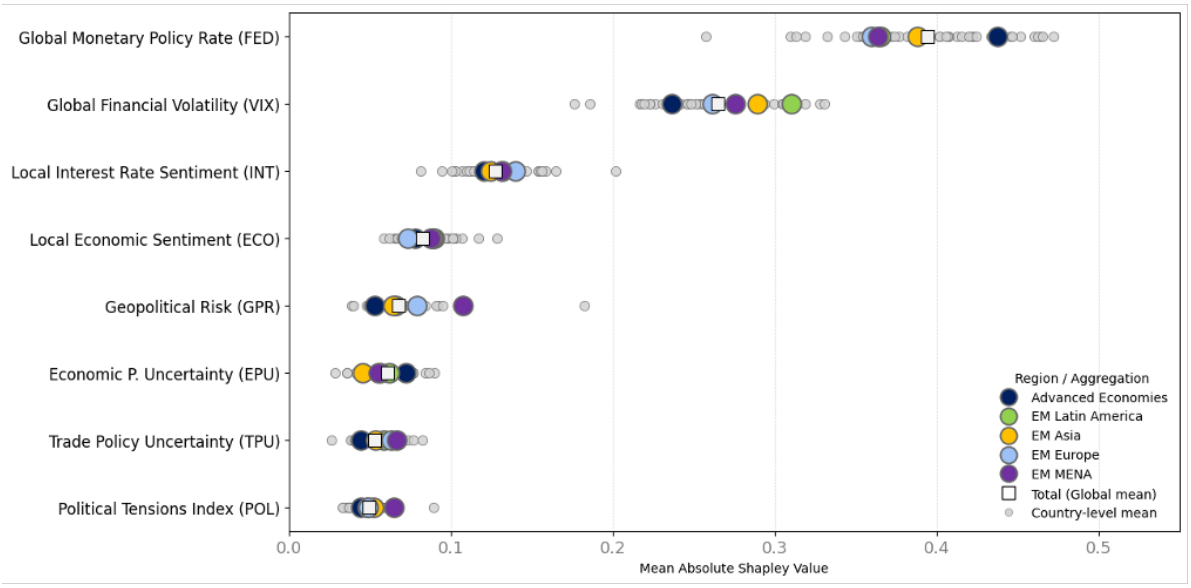

Notes: Mean absolute Shapley values for all predictors over 2018–2025, shown at the global, regional, and country levels. Country-level values are computed by averaging over all observations for each country; the global value is the unweighted mean across country means.

The second layer is domestic. Local interest-rate sentiment (INT) and economic sentiment (ECO) rank just below the global variables but display much greater cross-country dispersion, indicating that country-specific narratives are critical for differentiating sovereign spreads conditional on the global environment (Eichengreen et al., 2021). As noted in Section 3.2, these variables provide daily-frequency proxies for the core drivers of sovereign creditworthiness—growth prospects and the interest rate–growth differential—so their prominence in the Shapley ranking is consistent with the debt-sustainability fundamentals that anchor longer-horizon spread models.

The third layer is conditional. Geopolitical and policy-uncertainty indicators—GPR, EPU, and TPU—are smaller on average but become much more prominent in EM Europe and MENA, where exposure to geopolitical and geoeconomic risk is greater (Baker et al., 2016; Caldara et al., 2020), foreshadowing the state-dependent nonlinearities documented below.

4.3 Nonlinear Interactions and State Dependence

Pairwise Shapley–Taylor interaction values (Appendix Figure 8) show that global financial conditions are not only the largest main effects but also the dominant sources of nonlinear interaction. The largest and most pervasive interaction terms involve US2Y and the VIX, as well as interactions between US2Y and domestic interest-rate sentiment. By contrast, GPR and EPU rarely appear as large stand-alone drivers across the full sample, but they interact strongly with both global and domestic variables in EM Europe and MENA while remaining much weaker elsewhere. In the fitted model, geopolitical and policy-uncertainty variables matter primarily by changing how sovereign risk responds to the broader financial environment. This pattern provides a direct motivation for the channel grouping introduced in Section 3.2, where the global financial cycle block ($\mathcal{G}$) is defined as the set of variables that generate the strongest and most pervasive interactions.

The interaction surfaces reinforce this state dependence (Figure 2). When global financial conditions are benign, the joint contribution of geopolitical risk and policy uncertainty is relatively muted in most regions. By contrast, uncertainty becomes materially more important in high-volatility states (Bloom, 2009), and the strongest nonlinearities arise when elevated volatility coincides with tight U.S. rates: volatility shocks are powerfully amplified under tight monetary policy (Rey, 2013; Bruno and Shin, 2015) but partially contained under accommodative conditions (Bekaert et al., 2013). Geoeconomic or policy uncertainty, while often manageable in isolation, thus becomes a potent threat when it coincides with financial stress—a finding that motivates the four-channel decomposition developed next.

Figure 2: **State Dependence in Sovereign Risk: Two-Factor Interaction Surfaces**

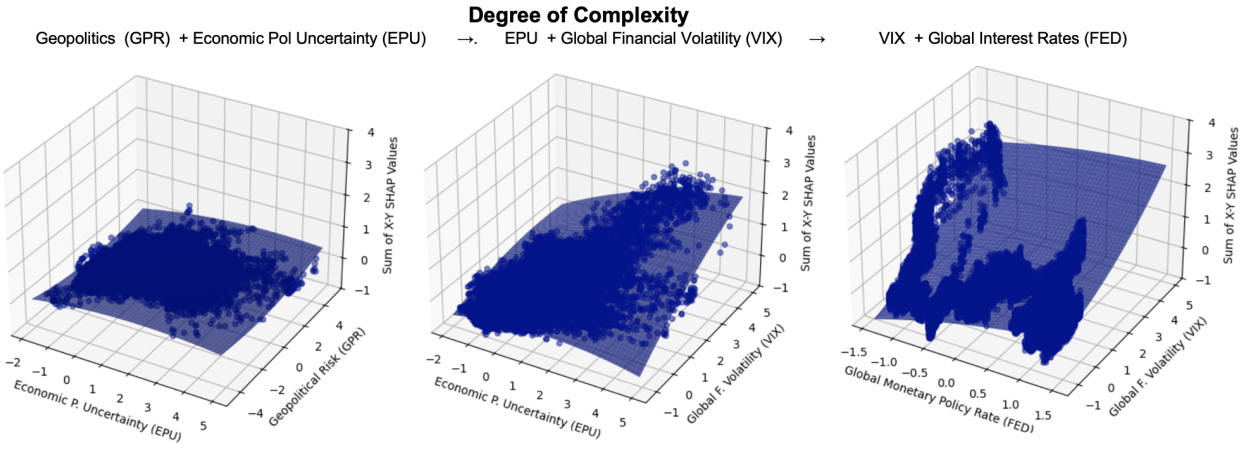

Notes: The figure illustrates the combined impact of key predictors on sovereign CDS spreads for Advanced Economies using two-factor SHAP dependence surfaces. Left panel: joint influence of Geopolitical Risk (GPR) and Economic Policy Uncertainty (EPU)—the surface is nearly flat, indicating low sensitivity when financial conditions are uncontrolled. Centre panel: joint contribution of EPU and Global Financial Volatility (VIX)—high uncertainty in a high-VIX environment is substantially more detrimental than either shock alone (Bloom, 2009). Right panel: joint effect of VIX and global monetary policy (US2Y)—the largest and most nonlinear increases in sovereign risk arise when volatility spikes coincide with tight monetary conditions (Rey, 2013; Bruno and Shin, 2015), but are partially contained under accommodative policy (Bekaert et al., 2013). See Section 4.3 for discussion.

Cross-country connectedness measures applied to the panel of daily Shapley attributions (Appendix C) yield the same broad message. Global financial variables are the dominant and persistent transmitters of cross-country co-movement, while geopolitical and policy-uncertainty shocks generate episodic synchronization that dissipates unless reinforced by

tighter financial conditions. The contrast between the Russia–Ukraine episode (simultaneous high Diebold–Yilmaz spillovers and high network density) and the Hamas–Israel episode (high density, low spillovers) is illustrative: the former combines system-wide transmission with dense synchronization, whereas the latter exhibits localized clustering. This pattern anticipates the shock-type taxonomy developed in the next section.

5 Transmission Anatomy of Geopolitical and Geoeconomic Shocks

Applying the four-channel decomposition, we begin by inspecting the raw attribution dynamics around each episode. Country-level Shapley paths around the Russia–Ukraine invasion (Appendix D Figure 10) are consistent with a staged propagation from geopolitical news to energy-related macro pressures and, with some delay, to interactions with global financial conditions. The remaining three episodes, shown in Appendix Figures 11–12, provide informative contrasts: the October 2023 Hamas–Israel war appears more regionally contained; the U.S. election and tariff episodes transmit less through the Direct channel and more through policy uncertainty, trade exposure, and global financial conditions, with the originator's own spreads rising through domestic policy uncertainty even as monetary easing compresses spreads abroad.

These raw attributions are informative but combine several mechanisms at once. To separate them, we apply the four-channel Shapley–Taylor decomposition to realized episode data, feeding observations through the estimated model—held fixed at its pre-episode parameters—and tracking daily channel contributions for the 42-country panel.[18] Three features organize the results. First, the configuration of channels differs systematically across geopolitical and geoeconomic episodes. Second, the cross-sectional distribution of each channel follows a distinct geographic or economic pattern. Third, the channels decay at different speeds. The remainder of this section develops these results in turn.

5.1 The Scissors Pattern

Figure 3 plots the cross-sectional average of the four Shapley–Taylor channels across all 42 countries for each episode.

Geopolitical episodes. In panel (a), the Russia–Ukraine invasion opens a clear "scissors": the Direct channel (red) jumps to roughly $+0.10$ within days as conflict exposure reprices default probability (Caldara and Iacoviello, 2022), while the GFC channel (blue) drops to approximately -0.05 as the global financial system partially absorbs the shock through the risk-taking channel (Rey, 2013; Bruno and Shin, 2015). The two move in opposite directions, so the total Shapley contribution rises only modestly—smaller than the Direct component alone because the financial-system response partly offsets the initial repricing. Panel (b) shows a similar but more muted pattern for Hamas–Israel: the Direct channel spikes, but the GFC response is much smaller in magnitude, consistent with a conflict whose spillovers remain more regionally contained. In both geopolitical episodes, the Uncertainty and Local channels are comparatively muted in cross-country mean terms at impact, even though country-level responses can be substantial for exposed sovereigns.

Geoeconomic episodes: transmission through financial and uncertainty channels. The geoeconomic episodes invert the picture. In panel (c), the Direct channel remains economically negligible throughout—the U.S. election does not reprice default probability. Instead, the GFC channel begins declining three months *before* the event as markets price in looser monetary policy (Miranda-Agrippino and Rey, 2020), and continues falling to roughly -0.08 by December, while the Uncertainty channel also contributes positively. Panel (d) is the sharpest illustration: the GFC plunges from near zero to approximately -0.12 within two weeks of the April 2025 tariff announcement. The Direct channel remains near zero—the tariff shock shifts expected monetary policy and risk appetite, not default probability.

Quantitative summary. Table 3 summarizes these patterns at one- and three-month horizons. The Direct channel exceeds the GFC at the panel level in both geopolitical episodes ($\varphi^{\text{dir}}_{1\text{m}} = +0.10$ vs. $\varphi^{\text{GFC}}_{1\text{m}} = -0.12$ for Russia–Ukraine; $+0.08$ vs. -0.01 for Hamas–Israel); the GFC dominates the Direct channel in both geoeconomic episodes. Taken together, geopolitical shocks load primarily on the Direct channel while provoking a partial GFC offset; geoeconomic shocks largely bypass the Direct channel and transmit through financial and uncertainty channels. Appendix Tables 6 and 7 report the complete country-level decomposition for all 42 economies, confirming that these patterns hold broadly across the panel.

[18] Country-level Shapley attribution dynamics for each episode are reported in Appendix E.

Figure 3: **Geopolitical vs. Geoeconomic Shocks: The Scissors Pattern**

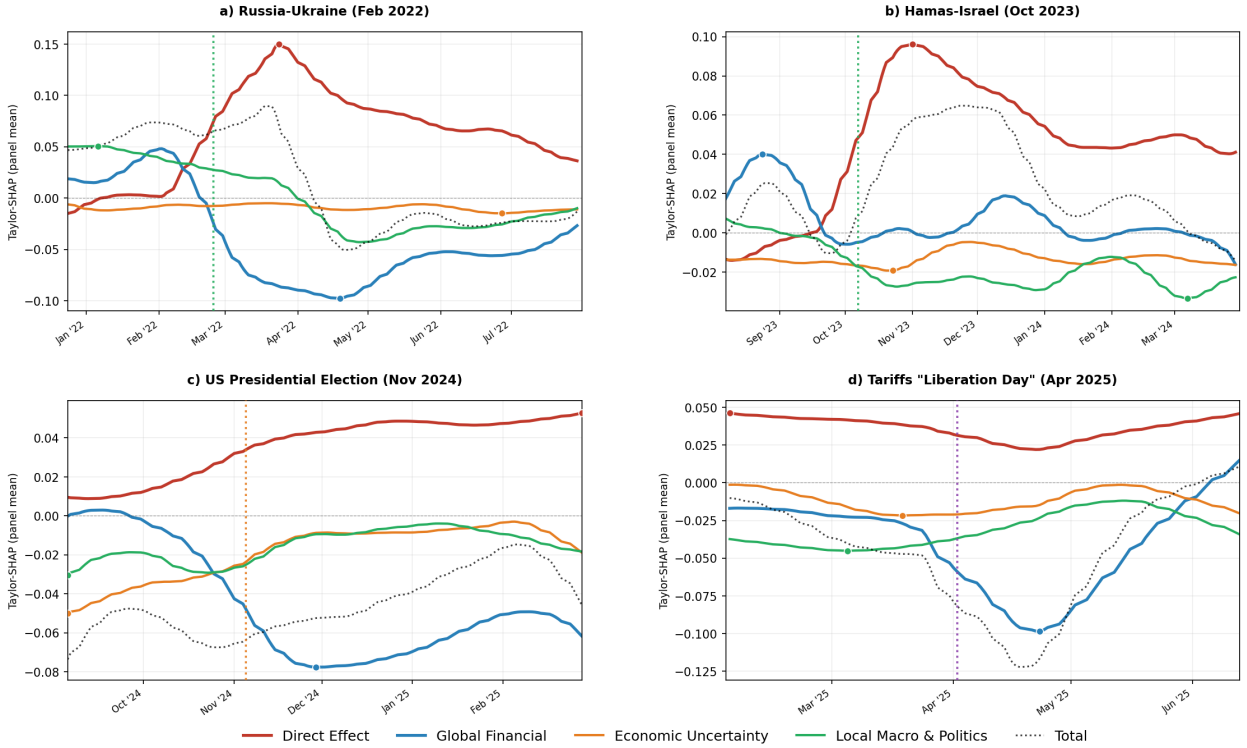

Notes: Each panel plots the cross-sectional average (42 countries) of the four Shapley–Taylor transmission channels (equation 3) for the indicator most directly associated with each episode: GPR for Russia–Ukraine (a) and Hamas–Israel (b), EPU for the U.S. Presidential Election (c), and TPU for the U.S. tariff shock (d). Direct (red): own Shapley–Taylor term φ^{dir}. Global Financial Cycle (blue): interactions with VIX and US2Y. Uncertainty (orange): interactions with EPU and TPU. Local (green): interactions with ECO, INT, POL, and regional indicators (REG). Dotted black line: total Shapley contribution. Vertical dashed lines mark the event date. All series are 28-day moving averages with a 7-day trailing smoother.

5.2 Country Heterogeneity

The scissors pattern describes the average response across countries. At the country level, transmission depends on the relative importance of two additional forces: exposure to the global financial cycle (φ^{GFC}) and the strength of domestic amplification (φ^{LOC}). By construction, these channels depend on different sets of predictors and need not move together.

Table 3 illustrates three distinct transmission modes within the geopolitical episodes. *Ukraine's* response is dominated by the GFC channel: $\varphi^{\text{GFC}}_{1\text{m}} = +0.66$, the largest single-channel value in the sample. Sanctions and market exclusion converted a geopolitical shock into a severe financial-intermediation event (Fernández-Villaverde et al., 2024), compounded by collapsing domestic sentiment ($\varphi^{\text{LOC}} = +0.48$). *Israel* presents a different balance: $\varphi^{\text{GFC}} = +0.32$ and $\varphi^{\text{LOC}} = +0.30$ contribute with broadly similar magnitudes, consistent with the joint activation of global risk-appetite sensitivity and domestic amplifiers (Gorodnichenko et al., 2025). The contrast is economically meaningful: Ukraine's crisis is primarily one of financial exclusion; Israel's reflects domestic strain in equal measure. *Poland* illustrates partial GFC compensation: the Direct-channel rise of $+0.15$ is materially offset by $\varphi^{\text{GFC}} = -0.10$, consistent with the idea that deep integration into European capital markets can cushion part of the initial shock.

The geoeconomic episodes reveal a different asymmetry. At the panel level, the tariff shock compresses spreads through the GFC as easier expected global financial conditions benefit most sovereigns. But the United States—the originator—is a partial exception. Its GFC contribution is a muted -0.02, while its Local channel registers $+0.07$: the policy uncertainty the originator created raises its own risk premia through the interaction of TPU with domestic sentiment and political tensions. The originator does not receive the same financial offset as the rest of the panel—consistent with evidence that geoeconomic instruments generate domestic risk premia (Clayton et al., 2025) and with the theoretical prediction of Pástor and Veronesi (2013) that uncertainty-generated risk premia are largest for the source country.

Table 3: Four-Channel Decomposition across Crisis Episodes: Impact and Persistence

	Nature of Shock	Short-Term Impact (Δ_{1m})					Persistence (Δ_{3m})				
		φ^{dir}	φ^{GFC}	φ^{UNC}	φ^{LOC}	φ^{tot}	φ^{dir}	φ^{GFC}	φ^{UNC}	φ^{LOC}	φ^{tot}
Panel A : Russia–Ukraine (GPR, Feb. 2022)											
Panel avg.	**Geopolitics** (Panel A)	+.10	-.12	.00	-.03	-.04	+.07	-.09	.00	-.03	-.05
Ukraine		+.13	+.66	-.02	+.48	+1.25	+.13	+.66	-.02	+.48	+1.25
Poland		+.15	-.10	+.04	+.06	+.14	+.11	-.02	+.04	+.06	+.20
Germany		+.25	-.24	+.02	+.06	+.09	+.15	-.11	+.01	+.05	+.10
Panel B : Hamas–Israel (GPR, Oct. 2023)											
Panel avg.	**Geopolitics** (Panel B)	+.08	-.01	+.01	-.02	+.06	+.06	-.02	.00	-.01	+.02
Israel		+.21	+.32	+.19	+.30	+1.02	+.21	+.34	+.16	+.33	+1.04
Egypt		+.27	+.08	+.08	+.07	+.51	+.21	-.07	+.01	-.06	+.09
Germany		+.09	-.15	-.02	+.02	-.06	+.09	-.18	-.04	.00	-.13
Panel C : U.S. Presidential Election (EPU, Nov. 2024)											
Panel avg.	**Economic Uncertainty** (Panel C)	+.03	-.06	+.03	+.01	+.01	+.04	-.06	+.03	+.01	+.01
USA		+.04	-.08	+.01	+.02	-.01	+.06	-.10	-.02	+.02	-.04
Mexico		+.03	-.03	+.01	.00	+.01	+.05	-.06	-.03	-.04	-.08
Germany		+.04	.00	+.06	+.04	+.15	+.05	-.04	+.05	+.04	+.10
Panel D : U.S. Tariffs / Liberation Day (TPU, Apr. 2025)											
Panel avg.	**Trade Uncertainty** (Panel D)	-.01	-.01	+.01	+.02	+.01	-.01	-.01	+.01	+.02	+.01
USA		.00	-.02	-.01	+.07	+.03	.00	-.02	-.01	+.07	+.03
India		-.01	-.10	-.03	+.02	-.12	-.01	-.10	-.03	+.02	-.12
Germany		.00	-.05	+.01	-.01	-.05	.00	-.05	+.01	-.01	-.05

Notes: Each cell reports $\Delta \equiv \bar{\varphi}^{post} - \bar{\varphi}^{pre}$ in standardized CDS units. Short-Term Impact: post-window = 1 month after event onset. Persistence: post-window = 3 months after event onset. Pre-event window = 3 months in both cases. Cell shading: $\Delta > +0.05$, $0.005 < \Delta \leq +0.05$, $|\Delta| \leq 0.005$, $-0.05 \leq \Delta < -0.005$, $\Delta < -0.05$. Values in σ-CDS units. *Panel avg.* = unweighted cross-country mean (42 countries). Germany appears in all panels as a common benchmark. 28-day moving averages applied to all series. φ^{LOC} includes interactions with local macro-political variables and regional indicators (ECO, INT, POL, REG; see equation 3).

5.3 Differential Persistence

If the Direct channel is associated with more persistent sovereign-specific repricing, while the GFC channel reflects more transitory financial adjustment, the two should fade at different speeds. Table 3 is consistent with that prediction. The Direct channel retains roughly two-thirds of its one-month value at three months in both geopolitical episodes: the underlying conflicts remain unresolved, so default-probability repricing persists (Caldara and Iacoviello, 2022; Boubaker et al., 2023). The GFC decays faster and can reverse sign, because risk-appetite shocks are mean-reverting (Bekaert et al., 2013; Bloom, 2009). The Local channel typically lies in between.

Egypt provides a useful illustration. At impact, all four channels contribute positively to spread widening: $\varphi^{tot}_{1m} = +0.51$. By three months, the GFC has reversed ($+0.08 \rightarrow -0.07$) and the Local channel has followed ($+0.07 \rightarrow -0.06$), pulling the total down to $+0.09$. But the Direct channel barely moved ($+0.27 \rightarrow +0.21$): Egypt's fundamental exposure to the conflict persisted even after the financial and domestic amplifiers faded. Mexico illustrates the opposite dynamic: its near-zero impact turns markedly negative at three months ($\varphi^{tot}_{3m} = -0.08$), as the GFC and Local channels accumulate while trade-policy uncertainty materialized into actual tariff actions (Caldara et al., 2020).

More broadly, the channels do not simply differ in sign and magnitude; they also evolve at different speeds. That temporal separation provides additional support for the taxonomy, because it is consistent with the idea that sovereign-specific repricing, financial adjustment, and domestic amplification are economically distinct components of the transmission process.

5.4 Cross-Sectional Fingerprints

The preceding subsections established that different shock types activate different channels over time. We now show that each activated channel also exhibits a distinct *cross-sectional* distribution, completing the transmission taxonomy.

Geopolitical shocks: gravity-like distance decay. If geopolitical shocks reprice default probability in proportion to conflict exposure, countries closer to the conflict should register larger Direct-channel effects—a gravity-style prediction familiar from the trade literature (Head and Mayer, 2014) and from work linking geographic proximity to financial contagion (Glick and Rose, 1999). Figure 4 evaluates this prediction by regressing the short-term direct effect on log great-circle distance:

$$\varphi_i^{\text{dir}} \;=\; \alpha \;+\; \beta \,\ln d_i \;+\; u_i \,, \tag{7}$$

where d_i is distance to Kyiv (left panel) or Tel Aviv (right panel).

Figure 4: **Direct Geopolitical Effects Decline with Distance from Conflict**

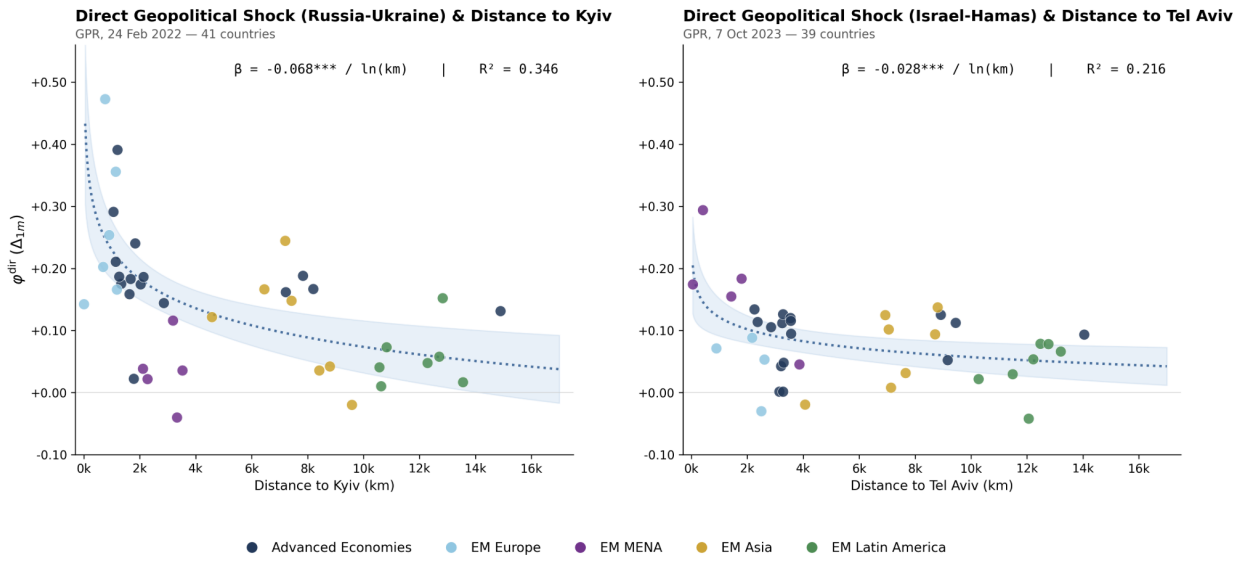

Notes: Each panel plots the one-month Direct-channel response $\varphi^{\text{dir}}(\Delta_{1\text{m}})$ against great-circle distance (km) from the national capital to the conflict epicenter (Kyiv, left panel; Tel Aviv, right panel). The decomposition follows equation (3). Left panel: 41 sovereigns (Russia–Ukraine, 24 February 2022; Ukraine at $d = 0$ plotted but excluded from log-distance OLS). Right panel: 39 sovereigns (Hamas–Israel, 7 October 2023). Dotted lines: OLS fitted values from equation (7); shaded bands: 95% confidence intervals. All values in within-country standard deviations of CDS spreads (σ-CDS). Jordan excluded due to insufficient pre-2023 CDS data. $^{***}\,p < 0.01$, $^{**}\,p < 0.05$, $^{*}\,p < 0.10$.

The Russia–Ukraine shock produces a steep, concave distance gradient ($\hat{\beta} = -0.068^{***}$ per log-km; $R^2 = 0.35$, $n = 40$). Countries within 1,200 km of Kyiv—Germany (+0.39), Czech Republic (+0.36), Austria (+0.29)—register Direct-channel responses two to three times the cross-sectional mean (+0.14); most Latin American sovereigns beyond 10,000 km fall below +0.08, though notable exceptions such as Argentina (+0.15) and Australia (+0.13) suggest that non-geographic linkages also play a role. The Hamas–Israel shock reveals a different geography: the slope is roughly half as steep ($\hat{\beta} = -0.028^{***}$; $R^2 = 0.22$, $n = 39$), with the four largest responses all belonging to MENA sovereigns within 2,000 km—Egypt (+0.29), Qatar (+0.18), Israel (+0.17), Saudi Arabia (+0.16). Both coefficients are significant at 1% under the log specification, which captures the concave decay pattern—steep attenuation near the epicenter, flattening at greater distances—better than the linear alternative. The cross-sectional footprint of the Direct channel is gravity-like in both cases, but much more pronounced for the more systemic of the two geopolitical shocks.

The regional component of the Local channel provides a sharp contrast. Appendix Figure 13 compares the Direct-channel and REG-within-LOC distance gradients for Russia–Ukraine side by side. Whereas the Direct channel exhibits significant gravity decay ($R^2 = 0.35$, $p < 0.001$), the regional component shows no distance relationship ($\hat{\beta} = -0.005$, $R^2 = 0.003$, $p = 0.72$), confirming that the regional group indicators do not proxy for geographic proximity to the conflict epicenter. This validates the absorption of REG into the Local channel: the proximity-based repricing captured by the Direct channel is structurally distinct from the regional comovement captured within LOC.

Policy-uncertainty shocks: global and simultaneous. The election episode leaves a different signature. Its most distinctive feature is the broad-based activation of the Uncertainty channel φ^{UNC}, which turns positive for a large share of countries at roughly the same time. At the panel level it registers +0.03 at both horizons, with a cross-country interquartile range of $[+0.01, +0.06]$; the appendix tables confirm positive values for France, Brazil, China, Germany

($+0.06$), and most other sovereigns.[19] This broad-based activation is much less visible in the other three episodes. In the tariff shock, φ^{UNC} is comparatively small; in the geopolitical episodes, it is limited mainly to the most exposed countries. The election episode therefore stands out not only by which channel activates, but also by how broadly and synchronously it does so—consistent with models in which political uncertainty generates correlated risk premia across all assets simultaneously (Pástor and Veronesi, 2012; Baker et al., 2016).

A three-way fingerprint. Together, these results complete the cross-sectional dimension of the taxonomy. Geopolitical shocks activate φ^{dir} with gravity-like structure. Trade shocks operate through φ^{GFC} in proportion to GFC exposure. Policy-uncertainty shocks activate φ^{UNC} broadly across countries. Each shock type has a distinct first-responder channel *and* a distinct cross-sectional distribution. This combination provides a useful empirical diagnostic for distinguishing the nature of a shock in real time.

In sum, the transmission anatomy rests on four related findings: (i) at the panel average, geopolitical shocks are characterized by a scissors pattern in which the Direct channel rises while the GFC channel provides a partial offset, whereas geoeconomic shocks load much more heavily on financial and uncertainty channels; (ii) country-level heterogeneity depends on the relative importance of GFC exposure and domestic amplification; (iii) the channels decay at different speeds, consistent with the idea that sovereign-specific repricing and financial adjustment are distinct components of the response; and (iv) each shock type leaves a distinct cross-sectional fingerprint. This is visible even for recurring benchmark countries. Germany, which appears in all four panels of Table 3, shifts from Direct-channel prominence under geopolitical shocks ($\varphi^{\mathrm{dir}} = +0.25$ for Russia–Ukraine) to GFC and Uncertainty prominence under geoeconomic shocks ($\varphi^{\mathrm{GFC}} = -0.05$, $\varphi^{\mathrm{UNC}} = +0.06$ for the election), suggesting that the nature of the shock plays a central role alongside country characteristics.

6 Econometric Validation via Local Projections

This section asks whether the four-channel taxonomy developed in Section 5 receives separate econometric support in panel local projections under the two identification strategies introduced in Section 3.3. The logic is simple. If the proposed channels capture economically meaningful differences in transmission, then they should respond differently to identified shocks even outside the machine-learning decomposition stage. Table 4 summarizes the main evidence at the 30-day horizon. The left panel reports the full-sample innovation LP; the right panel reports the narrative LP.

6.1 Full-Sample Innovation LP

The left panel of Table 4 reports the full-sample innovation LP. For GPR, EPU, and TPU innovations, the 30-day responses are small in magnitude and statistically imprecise across all four channels and all three control sets. No coefficient exceeds $\pm 0.005\sigma$ in absolute value, and none is significant at the 10% level. Appendix F confirms this pattern across the full horizon profile ($h = 0, \ldots, 90$).[20]

One interpretation of this null is that the full-sample design averages over many routine news days on which channel responses are weak, offsetting, or both. In particular, if geopolitical shocks raise the Direct channel while simultaneously lowering the GFC channel, the average response can be small even when episode-specific movements are economically meaningful. Low power and attenuation from state averaging may therefore be especially important in this setting. The null does not by itself validate the taxonomy, but it provides a clear reason to turn to the narrative design, which isolates large dated episodes where the proposed channels should separate most sharply.

6.2 Narrative LP: Four Crisis Episodes

In sharp contrast to the full-sample null, the narrative LP detects large and statistically significant aggregate CDS responses: Russia–Ukraine generates $+0.54\sigma$ at $h = 30$ ($p < 0.01$), rising to $\sim 1.5\sigma$ by $h = 90$; Hamas–Israel produces -0.18σ ($p < 0.05$), consistent with flight-to-quality compression for non-MENA sovereigns; the U.S. election raises CDS by $+0.11\sigma$ ($p < 0.10$) with a gradual 60-day build-up; and "Liberation Day" tariffs produce a hump-shaped

[19] The cross-country standard deviation of $\varphi^{\mathrm{UNC}}_{1\mathrm{m}}$ is 0.02 for the election episode—roughly one-third of the corresponding dispersion for φ^{dir} in the Russia–Ukraine episode (0.07). The narrow spread confirms that the Uncertainty channel activates broadly rather than selectively.

[20] Despite the aggregate null, channel-level IRFs produce qualitative sign patterns consistent with four of the taxonomy's five predictions at the 68% level, though none reaches conventional significance: (i) GPR innovations raise φ^{dir} by $\sim +0.015\sigma$ on impact for $\sim$20 days; (ii) TPU innovations produce φ^{dir} indistinguishable from zero at every horizon; (iii) EPU innovations preferentially activate φ^{UNC}. The exception—the negative GFC-channel response to geopolitical shocks (the scissors)—requires the narrative LP to recover. See Appendix F for horizon-by-horizon detail.

Table 4: **Local-Projection Validation of the Channel Taxonomy**

		Full-Sample Innovation LP			Narrative LP		
		(A) Baseline	(B) Global	(C) Extended	(A) Baseline	(B) Global	(C) Extended
Episode	**Channel**	$\hat{\beta}$ Sig.	$\hat{\beta}$ Sig.	$\hat{\beta}$ Sig.	$\hat{\beta}$ Sig.	$\hat{\beta}$ Sig.	$\hat{\beta}$ Sig.
Russia–Ukraine GPR, Feb. 2022 *Geopolitical*	φ^{dir}	$+.005$ –	$+.005$ –	$+.005$ –	$+.122$ ***	$+.121$ ***	$+.125$ ***
	φ^{GFC}	$-.001$ –	$-.001$ –	$-.001$ –	$-.102$ ***	$-.104$ ***	$-.102$ ***
	φ^{UNC}	$-.000$ –	$-.000$ –	$-.000$ –	$-.009$ *	$-.010$ *	$-.009$ *
	φ^{LOC}	$-.004$ –	$-.004$ –	$-.004$ –	$-.018$ –	$-.023$ –	$-.023$ –
Hamas–Israel GPR, Oct. 2023 *Geopolitical*	φ^{dir}	$+.005$ –	$+.005$ –	$+.005$ –	$+.071$ ***	$+.072$ ***	$+.068$ ***
	φ^{GFC}	$-.001$ –	$-.001$ –	$-.001$ –	$+.003$ –	$+.000$ –	$-.000$ –
	φ^{UNC}	$-.000$ –	$-.000$ –	$-.000$ –	$+.006$ –	$+.006$ –	$+.006$ –
	φ^{LOC}	$-.004$ –	$-.004$ –	$-.004$ –	$-.017$ –	$-.018$ –	$-.019$ –
U.S. Election EPU, Nov. 2024 *Geoeconomic*	φ^{dir}	$+.002$ –	$+.002$ –	$+.003$ –	$+.013$ ***	$+.013$ ***	$+.015$ ***
	φ^{GFC}	$+.002$ –	$+.002$ –	$+.004$ –	$-.044$ ***	$-.046$ ***	$-.046$ ***
	φ^{UNC}	$+.001$ –	$+.001$ –	$+.001$ –	$+.021$ ***	$+.021$ ***	$+.024$ ***
	φ^{LOC}	$+.000$ –	$+.000$ –	$+.000$ –	$+.016$ ***	$+.015$ ***	$+.017$ ***
"Liberation Day" TPU, Apr. 2025 *Geoeconomic*	φ^{dir}	$-.001$ –	$-.001$ –	$-.002$ –	$-.008$ ***	$-.009$ ***	$-.016$ ***
	φ^{GFC}	$-.001$ –	$-.001$ –	$-.001$ –	$-.015$ –	$-.019$ *	$-.028$ ***
	φ^{UNC}	$+.001$ –	$+.001$ –	$+.001$ –	$+.026$ ***	$+.026$ ***	$+.034$ ***
	φ^{LOC}	$+.000$ –	$+.000$ –	$-.001$ –	$+.034$ **	$+.032$ **	$+.023$ *

Notes: Each cell reports the cumulative impulse response at horizon $h = 30$ days. Coefficients rounded to three decimal places. *Full-sample innovation LP*: panel local projection with country-specific AR(5) innovations; Driscoll–Kraay SE with bandwidth $\max(20, h)$, country and time FE, 5 lags. *Narrative LP*: panel local projection with $\pm$3-day event dummies; Driscoll–Kraay SE with country FE. Controls: (A) none; (B) VIX, US2Y; (C) VIX, US2Y, ECO, INT, POL, EPU, TPU. $^{***}\,p < 0.01$, $^{**}\,p < 0.05$, $^{*}\,p < 0.10$; – = not significant at 10%. Cell shading indicates significance level of the Narrative LP estimate: $p < 0.01$, $p < 0.05$, $p < 0.10$. Because the full-sample innovation LP is estimated by shock type rather than by narrative episode, the GPR-based coefficients are repeated in the two geopolitical rows to facilitate comparison with the narrative panel. GPR = Geopolitical Risk, EPU = Economic Policy Uncertainty, TPU = Trade Policy Uncertainty, US2Y = U.S. two-year Treasury yield.

response peaking at $+0.15\sigma$ ($p < 0.01$) before partially reversing.[21] The contrast with the innovation null resolves an apparent puzzle: geopolitical shocks have large effects on sovereign spreads, but these effects are concentrated in discrete crisis episodes that are washed out when averaged over routine news-innovation days.

Channel decomposition. Figure 5 plots the full horizon profiles for the four channels under the narrative design. Table 4 reports the corresponding cumulative responses at $h = 30$ under the three control sets. For interpretation, specification (B) is our preferred baseline because it conditions on global financial variables while remaining parsimonious; specifications (A) and (C) show that the results are stable to omitting or extending the control set. Four results stand out.

E1—Russia–Ukraine (GPR shock). The Direct channel rises sharply ($\hat{\beta}^{h=30} = +0.121$, $p < 0.01$) while the GFC channel moves in the opposite direction (-0.104, $p < 0.01$), recovering the scissors pattern at the 1% significance level. That the scissors does not appear in the full-sample LP is consistent with it being a crisis phenomenon requiring a shock large enough to simultaneously reprice default probabilities and trigger rebalancing of global financial conditions. The horizon profiles in Figure 5 further suggest that the Direct and GFC channels decay at different speeds, with the Direct response more persistent—independently confirming that fundamental repricing and financial amplification are distinct forces (Bekaert et al., 2013; Bloom et al., 2018).[22]

[21] Full aggregate impulse-response paths are reported in Appendix F.

[22] We also estimate a threshold specification and a smooth-transition variant following Auerbach and Gorodnichenko (2012) and Ramey and Zubairy (2018). Neither recovers the scissors using full-sample innovation shocks, because the GFC channel already incorporates the GPR $\times$ VIX interaction by construction and the linear LP averages over states. See Appendix B.

Figure 5: **Channel Impulse Responses from Narrative Local Projections**

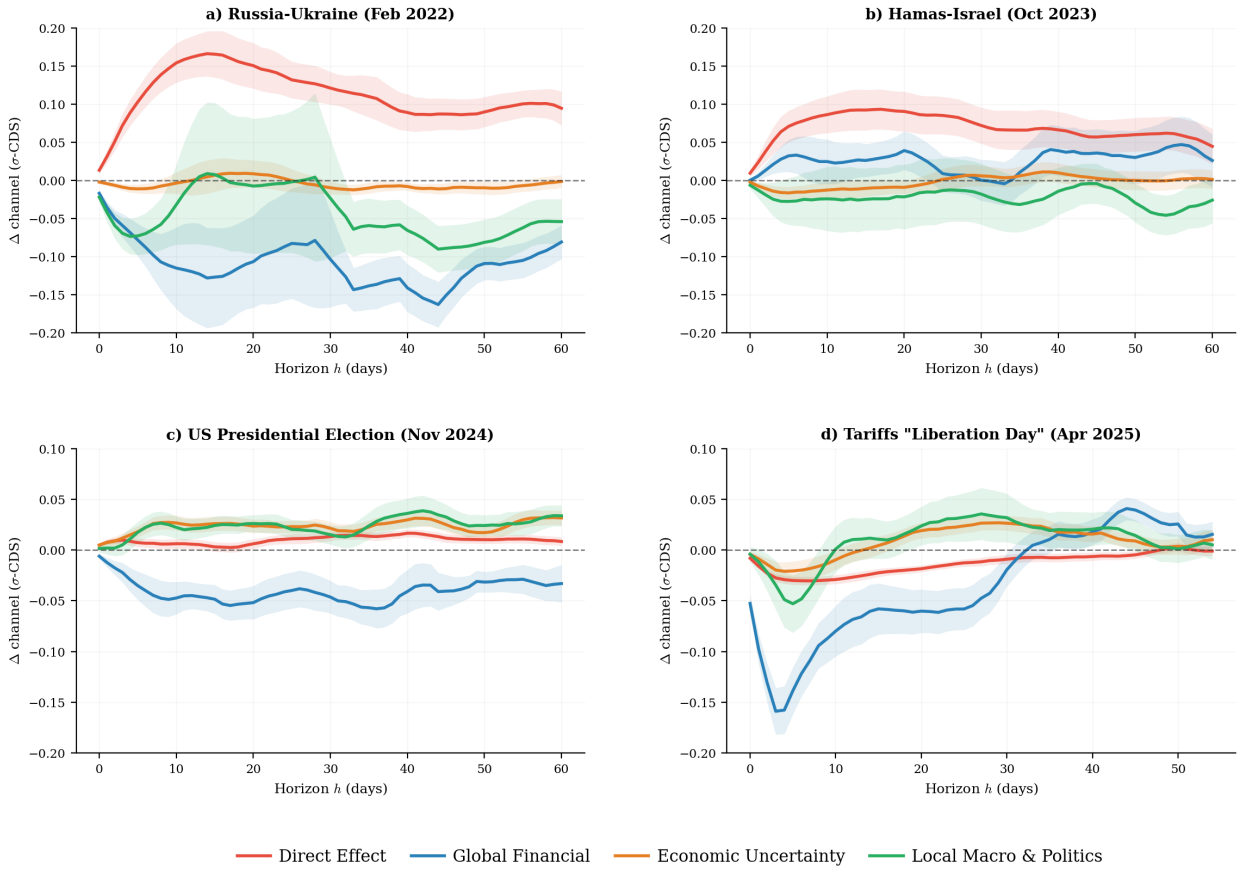

Notes: Each panel plots cumulative impulse responses of the four Shapley–Taylor channels—Direct (φ^{dir}, red), GFC (φ^{GFC}, blue), Uncertainty (φ^{UNC}, orange), and Local (φ^{LOC}, green)—from narrative local projections with $\pm$3-day event dummies at horizons $h = 0, \ldots, 60$ days. Specification (B): VIX and US2Y controls; country FE; Driscoll–Kraay SE. Shaded bands: 90% confidence intervals.

E2—Hamas–Israel (GPR shock). The Direct channel activates ($+0.072$, $p < 0.01$) at roughly half the E1 magnitude, consistent with a more regionally contained conflict. The GFC channel is indistinguishable from zero ($+0.000$), confirming that localized geopolitical shocks reprice default probability without triggering a global financial offset. The E1–E2 contrast supports a distinction between geopolitical shocks that become globally systemic and those that remain more localized: Russia–Ukraine ($\varphi^{\mathrm{dir}} = +0.121$, $\varphi^{\mathrm{GFC}} = -0.104$) produces a textbook scissors; Hamas–Israel ($\varphi^{\mathrm{dir}} = +0.072$, $\varphi^{\mathrm{GFC}} \approx 0$) does not.This is the single unconfirmed prediction among the sixteen event–channel tests: the regionally contained nature of the conflict did not trigger the global financial offset that characterizes systemic geopolitical shocks.

E3—U.S. Presidential Election (EPU shock). The Uncertainty channel is the largest positive response ($+0.021$, $p < 0.01$), the GFC is significantly negative (-0.046, $p < 0.01$), and both Direct ($+0.013$) and Local ($+0.015$) channels are positive and significant. The key point is not that the Direct channel is literally absent, but that it is secondary to the Uncertainty and GFC responses. This multi-channel activation—with Uncertainty as first responder—is the broad-based fingerprint that distinguishes policy-uncertainty shocks from both geopolitical and trade-policy episodes.

E4—"Liberation Day" Tariffs (TPU shock). The Uncertainty ($+0.026$, $p < 0.01$) and Local ($+0.032$, $p < 0.05$) channels are the dominant positive contributors, while the GFC drops on impact (-0.019, $p < 0.10$). The Direct channel response (-0.009, $p < 0.01$) is statistically detectable but economically small relative to the dominant channels. The evidence is therefore more consistent with a shock that transmits through policy uncertainty, domestic amplification, and financial conditions than with one that primarily reprices sovereign-specific default risk. The comparison with E1 is instructive: $\varphi^{\mathrm{dir}} = +0.121$ for Russia–Ukraine versus $\varphi^{\mathrm{dir}} = -0.009$ for "Liberation Day"—an

Figure 6: **Placebo Falsification: Actual Channel Responses vs. Random-Date Envelope.**

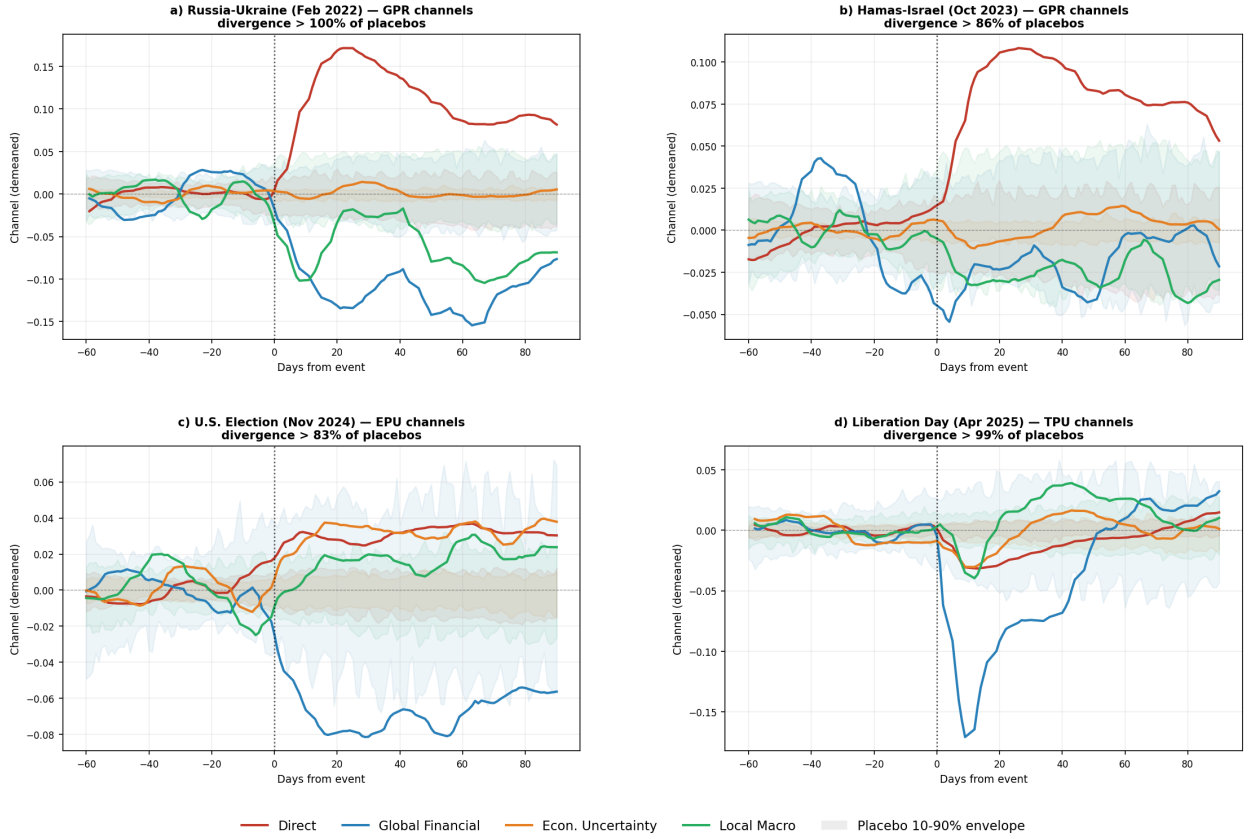

Notes: Each panel plots the cross-country mean of the four demeaned channel series (φ^{dir}, φ^{gfc}, φ^{unc}, φ^{loc}) in a $[-60, +90]$-day window around the event date (solid lines) against the 10–90% envelope from 100 randomly drawn non-event dates (shaded bands). Each episode uses its driver-specific Shapley–Taylor decomposition: GPR for Russia–Ukraine and Hamas–Israel; EPU for the U.S. Presidential Election; TPU for the Liberation Day tariff shock. Panel titles report the percentile of the placebo distribution exceeded by the actual event's maximum post-event channel divergence. Channel series smoothed with a 7-day trailing moving average and demeaned over the pre-event window.

order-of-magnitude difference establishing that geopolitical and geoeconomic shocks generate qualitatively different Direct-channel responses.

Stability and scorecard. The qualitative pattern is stable across the three control sets. Moving from specification (A) to specification (C) changes point estimates only modestly (e.g., the E1 Direct channel moves from $+0.122$ to $+0.125$; the E1 GFC from -0.102 to -0.102) and leaves the main sign pattern intact. Overall, the narrative LP supports 15 of 16 event–channel predictions: φ^{dir} activates for both geopolitical events (E1, E2) but is economically negligible for the geoeconomic event (E4); φ^{UNC} dominates for the political-uncertainty event (E3); and the scissors is recovered at the 1% significance level for E1. Because this validation exercise is separate from model selection and from the Shapley decomposition itself, it provides complementary econometric support for the proposed interpretation of the channels.

Placebo falsification. To verify that the scissors pattern is event-specific, we draw 100 random non-event dates and construct the 10–90% envelope of channel responses in a $[-60, +90]$-day window around each placebo date, using the driver-specific Shapley–Taylor decomposition for each episode (GPR for geopolitical events; EPU and TPU for geoeconomic events). All four episodes produce channel divergence well outside this envelope: Russia–Ukraine exceeds 100% of placebos, Liberation Day 99%, Hamas–Israel 86%, and the U.S. Presidential Election 83%. Crucially, the channels that exit the placebo bands differ across shock types in the direction the taxonomy predicts. Figures 14–17 in Appendix F.1 decompose each episode channel by channel. For geopolitical episodes, the Direct channel exits the 90% band upward while the GFC channel exits downward, and the Uncertainty channel remains inside the placebo range. For geoeconomic episodes, the pattern reverses: the GFC channel dominates the departure, the Uncertainty channel exits the envelope (upward for the Election, consistent with EPU-driven repricing), while the Direct channel stays within or moves opposite to the geopolitical case.

Block bootstrap validation. Because the channel decomposition treats Shapley–Taylor values as observed regressors, the Driscoll–Kraay standard errors in Table 4 do not account for estimation uncertainty in the first-stage ML model. We address this with a generated-regressor block bootstrap ($B = 200$) that, in each replication, jointly re-estimates the Multilayer Random Forest tree, recomputes the Shapley–Taylor decomposition, and re-runs the panel local projection. Appendix Figure 18 overlays the resulting 90% confidence intervals on the baseline Driscoll–Kraay bands. The graph yields two findings. First, bootstrap standard errors are uniformly smaller—the median SE ratio (bootstrap/DK) is 0.05 at $h = 30$—indicating that the channel decomposition is stable across re-estimations and that our baseline inference is conservative. Second, no channel that is significant under Driscoll–Kraay loses significance under the bootstrap; if anything, several impact responses ($h = 0$) that fall short of conventional thresholds under DK become significant once generated-regressor uncertainty (Pagan, 1984) is properly internalized. Together, these results confirm that the transmission taxonomy documented in Sections 3.2–5.2 is not an artifact of a single ML partition.

7 Conclusion

The central result of this paper is a scissors pattern in sovereign risk transmission. Geopolitical shocks raise sovereign CDS spreads primarily through a direct channel associated with sovereign-specific repricing, while the GFC channel moves in the opposite direction and partly offsets that increase. Geoeconomic shocks display a different configuration: the direct channel is comparatively small, and the response operates mainly through financial conditions, policy uncertainty, and domestic amplification.

Three validation exercises support this taxonomy. Narrative local projections recover the scissors at the 1% significance level for Russia–Ukraine and confirm 15 of 16 event–channel predictions across four crisis episodes. A placebo falsification using driver-specific decompositions shows that all four episodes exceed at least 83% of random non-event dates, with different channels exiting the envelope for each shock type. Direct geopolitical effects decay with distance in a gravity-style pattern ($R^2 = 0.35$ for Russia–Ukraine under the log-distance specification; both episodes significant at 1%), while the regional component of the local channel shows no distance gradient ($R^2 = 0.003$), validating the four-channel design. A further finding is an originator penalty: geoeconomic-shock originators face widening spreads through the local channel even as monetary easing compresses spreads abroad.

This distinction carries policy implications. When spread widening is mediated mainly by the GFC, central-bank liquidity provision and swap lines can help stabilize funding conditions (Bahaj and Reis, 2022). When it reflects sovereign-specific repricing, liquidity tools are unlikely to be sufficient; the appropriate margin of adjustment is diplomatic de-escalation, fiscal correction, or institutional strengthening. Monitoring high-frequency news-based indicators is most useful not simply because it signals that risk is rising, but because it can help identify *which channel* is driving that rise. As geoeconomic tensions become more prominent, the balance of transmission is likely to shift toward channels the standard central-bank toolkit was not designed to address—the Liberation Day episode operated almost entirely outside the direct channel, yet generated substantial spread movements that conventional liquidity facilities can only partially offset.

The channel measures are constructed from a fitted nonlinear model and should be interpreted as model-based decompositions rather than direct structural objects; the local projection, placebo, and block-bootstrap layers mitigate but do not fully resolve this concern. Whether the taxonomy extends to other maturities or non-sovereign asset classes remains open. A natural next step is to embed the four-channel decomposition in the geoeconomic framework of Clayton et al. (2026), linking the empirical channel assignments to the structural trade-offs their model formalizes. A second direction is to exploit forward-looking channel interactions—how today's channel configuration predicts future spread movements—to develop real-time monitoring tools for sovereign risk surveillance. Third, the nonlinear dependence between channels documented here suggests that modeling sovereign CDS as a state-dependent function of the four channels, rather than as a linear combination, may yield both forecasting gains and deeper insight into the conditions under which geopolitical shocksbecome systemic.

Taken together, the central conclusion is that geopolitical and geoeconomic shocks move sovereign spreads through systematically different channels, and recognizing that difference is essential for both economic interpretation and policy design.

References

Ahir, H., Bloom, N., and Furceri, D. (2018). The world uncertainty index. *Brookings Papers on Economic Activity*, pages 343–400.

Ahn, D. P. and Ludema, R. D. (2020). The sword and the shield: The economics of targeted sanctions. *European Economic Review*, 130:103578.

Aiyar, S., Presbitero, A. F., and Ruta, M. (2023). Geoeconomic fragmentation and the future of multilateralism. Staff Discussion Note SDN/2023/001, International Monetary Fund.

Aizenman, J., Hutchison, M., and Jinjarak, Y. (2013). What is the risk of European sovereign debt defaults? Fiscal space, CDS spreads and market pricing of risk. *Journal of International Money and Finance*, 34:37–59.

Alonso-Alvarez, I., Diakonova, M., and Pérez, J. J. (2025). Rethinking GPR: The sources of geopolitical risk. Documentos de Trabajo 2522, Banco de España.

Antolín-Díaz, J. and Rubio-Ramírez, J. F. (2018). Narrative sign restrictions for SVARs. *American Economic Review*, 108(10):2802–2829.

Athey, S. and Imbens, G. W. (2019). Machine learning methods that economists should know about. *Annual Review of Economics*, 11:685–725.

Auerbach, A. J. and Gorodnichenko, Y. (2012). Measuring the output responses to fiscal policy. *American Economic Journal: Economic Policy*, 4(2):1–27.

Augustin, P., Subrahmanyam, M. G., Tang, D. Y., and Wang, S. Q. (2022). Sovereign credit risk. *Journal of Financial Economics*, 146(2):431–453.

Bahaj, S. and Reis, R. (2022). Central banking in challenging times: Central bank liquidity lines. *American Economic Journal: Macroeconomics*, 14(2):110–150.

Baker, S. R., Bloom, N., and Davis, S. J. (2016). Measuring economic policy uncertainty. *Quarterly Journal of Economics*, 131(4):1593–1636.

Bauer, M. D., Bernanke, B. S., and Milstein, E. (2023). Risk appetite and the risk-taking channel of monetary policy. *Journal of Economic Perspectives*, 37(1):157–186.

Bekaert, G., Hoerova, M., and Lo Duca, M. (2013). Risk, uncertainty and monetary policy. *Journal of Monetary Economics*, 60(7):771–788.

Bloom, N. (2009). The impact of uncertainty shocks. *Econometrica*, 77(3):623–685.

Bloom, N., Floetotto, M., Jaimovich, N., Saporta-Eksten, I., and Terry, S. J. (2018). Really uncertain business cycles. *Econometrica*, 86(3):1031–1065.

Bondarenko, Y., Lewis, V., Rottner, M., and Schüler, Y. (2024). Geopolitical risk perceptions. *Journal of International Economics*, 152:104005.

Boubaker, S., Goodell, J. W., Kumar, S., and Sureka, R. (2023). Geopolitical risk and energy stock performance: Evidence from the Russia–Ukraine conflict. *Journal of Commodity Markets*, 30:100325.

Breiman, L. (2001). Random forests. *Machine Learning*, 45(1):5–32.

Bruno, V. and Shin, H. S. (2015). Capital flows and the risk-taking channel of monetary policy. *Journal of Monetary Economics*, 71:119–132.

Caldara, D. and Iacoviello, M. (2022). Measuring geopolitical risk. *American Economic Review*, 112(4):1194–1225.

Caldara, D., Iacoviello, M., Molligo, P., Prestipino, A., and Raffo, A. (2020). The economic effects of trade policy uncertainty. *Journal of Monetary Economics*, 109:38–59.

Calvo, G. A., Leiderman, L., and Reinhart, C. M. (1996). Inflows of capital to developing countries in the 1990s. *Journal of Economic Perspectives*, 10(2):123–139.

Chernozhukov, V., Hansen, C., Kallus, N., Spindler, M., and Syrgkanis, V. (2024). Applied causal inference powered by ml and ai.

Clayton, C., Coppola, A., Maggiori, M., and Schreger, J. (2025). Geoeconomic pressure. Working Paper 34020, National Bureau of Economic Research.

Clayton, C., Maggiori, M., and Schreger, J. (2026). A framework for geoeconomics. *Econometrica*, 94(1):105–136.

Diebold, F. X. and Yilmaz, K. (2014). On the network topology of variance decompositions: Measuring the connectedness of financial firms. *Journal of Econometrics*, 182(1):119–134.

Driscoll, J. C. and Kraay, A. C. (1998). Consistent covariance matrix estimation with spatially dependent panel data. *Review of Economics and Statistics*, 80(4):549–560.

Du, W., Im, J., and Schreger, J. (2018). The dollar, bank funding and global financial conditions. *Journal of Finance*, 73(2):537–586.

Eichengreen, B., Hausmann, R., and Panizza, U. (2021). Original sin redux: A modern assessment of emerging-market vulnerabilities. *Journal of International Money and Finance*, 110:102280.

Fernández-Villaverde, J., Li, Y., Xu, L., and Zanetti, F. (2025). Charting the uncharted: The (un)intended consequences of oil sanctions and dark shipping. Working Paper 33486, National Bureau of Economic Research.

Fernández-Villaverde, J., Mineyama, T., and Song, D. (2024). Are we fragmented yet? measuring geopolitical fragmentation and its causal effects. Working Paper 32638, National Bureau of Economic Research.

Friedman, J. H. (2001). Greedy function approximation: A gradient boosting machine. *Annals of Statistics*, 29(5):1189–1232.

Gelos, R. G., Sahay, R., and Sandleris, G. (2011). Sovereign borrowing by developing countries: What determines the bond spread? *Journal of Development Economics*, 96(2):273–282.

Gentzkow, M., Kelly, B., and Taddy, M. (2019). Text as data. *Journal of Economic Literature*, 57(3):535–574.

Glick, R. and Rose, A. K. (1999). Contagion and trade: Why are currency crises regional? *Journal of International Money and Finance*, 18(4):603–617.

Gopinath, G., Gourinchas, P.-O., Presbitero, A. F., and Topalova, P. (2025). Changing global linkages: A new cold war? *Journal of International Economics*, 153(C).

Gorodnichenko, Y., Georgarakos, D., Kenny, G., and Coibion, O. (2025). The impact of geopolitical risk on consumer expectations and spending. Working Paper 34195, National Bureau of Economic Research.

Gu, S., Kelly, B. T., and Xiu, D. (2020). Empirical asset pricing via machine learning. *Review of Financial Studies*, 33(5):2223–2273.

Hassan, T. A., Hollander, S., van Lent, L., and Tahoun, A. (2019). Firm-level political risk: Measurement and effects. *Quarterly Journal of Economics*, 134(4):2135–2202.

Head, K. and Mayer, T. (2014). Gravity equations: Workhorse, toolkit, and cookbook. In Gopinath, G., Helpman, E., and Rogoff, K., editors, *Handbook of International Economics*, volume 4, pages 131–195. Elsevier.

Hoerl, A. E. and Kennard, R. W. (1970). Ridge regression: Biased estimation for nonorthogonal problems. *Technometrics*, 12(1):55–67.

Jordà, O. (2005). Estimation and inference of impulse responses by local projections. *American Economic Review*, 95(1):161–182.

LeCun, Y., Bengio, Y., and Hinton, G. (2015). Deep learning. *Nature*, 521(7553):436–444.

Leetaru, K. and Schrodt, P. A. (2013). GDELT: Global data on events, location, and tone, 1979–2012. Technical Report Version 1.0, GDELT Project. Presented at the International Studies Association Annual Convention, San Francisco, CA.

Longstaff, F. A., Pan, J., Pedersen, L. H., and Singleton, K. J. (2011). How sovereign is sovereign credit risk? *American Economic Journal: Macroeconomics*, 3(2):75–103.

Lundberg, S. M. and Lee, S.-I. (2017). A unified approach to interpreting model predictions. In *Advances in Neural Information Processing Systems*, volume 30, pages 4765–4774. Curran Associates, Inc.

Maggiori, M., Neiman, B., and Schreger, J. (2020). International currencies and capital allocation. *Journal of Political Economy*, 128(6):2019–2066.

Miranda-Agrippino, S. T. and Rey, H. (2020). U.S. monetary policy and the global financial cycle. *Review of Economic Studies*, 87(6):2754–2776.

Mohr, C. and Trebesch, C. (2025). Geoeconomics. Kiel Working Papers 2279, Kiel Institute for the World Economy.

Mullainathan, S. and Spiess, J. (2017). Machine learning: An applied econometric approach. *Journal of Economic Perspectives*, 31(2):87–106.

Novta, N. and Pugacheva, E. (2021). Geopolitical risks and capital flows to emerging markets. *Journal of International Money and Finance*, 115:102391.

Pagan, A. (1984). Econometric issues in the analysis of regressions with generated regressors. *International Economic Review*, 25(1):221–247.

Pan, J. and Singleton, K. J. (2008). Default and recovery implicit in the term structure of sovereign CDS spreads. *Journal of Finance*, 63(5):2345–2384.

Pástor, V. and Veronesi, P. (2012). Uncertainty about government policy and stock prices. *Journal of Finance*, 67(4):1219–1264.

Pástor, V. and Veronesi, P. (2013). Political uncertainty and risk premia. *Journal of Political Economy*, 121(1):36–72.

Pesaran, M. H. and Shin, Y. (1998). Generalized impulse response analysis in linear multivariate models. *Economics Letters*, 58(1):17–29.

Plagborg-Møller, M. and Wolf, C. K. (2021). Local projections and VARs estimate the same impulse responses. *Econometrica*, 89(2):955–980.

Ramey, V. A. and Zubairy, S. (2018). Government spending multipliers in good times and in bad: Evidence from us historical data. *Journal of Political Economy*, 126(2):850–901.

Rey, H. (2013). Dilemma not trilemma: The global financial cycle and monetary policy independence. In *Proceedings of the Jackson Hole Economic Policy Symposium*, pages 285–333.

Romer, C. D. and Romer, D. H. (2010). The macroeconomic effects of tax changes: Estimates based on a new measure of fiscal shocks. *American Economic Review*, 100(3):763–801.

Shapley, L. S. (1953). A value for n-person games. In *Contributions to the Theory of Games*, volume 2, pages 307–317. Princeton University Press.

Swanson, E. T. (2021). Measuring the effects of federal reserve forward guidance and asset purchases on financial markets. *Journal of Monetary Economics*, 118:32–53.

Tibshirani, R. (1996). Regression shrinkage and selection via the lasso. *Journal of the Royal Statistical Society: Series B (Methodological)*, 58(1):267–288.

Varian, H. R. (2014). Big data: New tricks for econometrics. *Journal of Economic Perspectives*, 28(2):3–28.

Zou, H. and Hastie, T. (2005). Regularization and variable selection via the elastic net. *Journal of the Royal Statistical Society: Series B (Statistical Methodology)*, 67(2):301–320.

A APPENDIX A:The data

This Appendix details data availability and percentile distributions by country (Appendix A.1), the construction of news indicators (Appendix A.2) and LOESS Unconditional Scatters.

A.1 Data availability by country

The following table presents country-specific data availability together with descriptive statistics summarizing the distribution of the main variables. For each country, the start and end dates of the available sample are reported. To characterize the distribution, we provide the 25th and 75th percentiles (p25 and p75), which capture the inter-quartile range where the central 50% of observations lie, for each of the described variables in the data section.

Table 5: **Country-specific sample periods and interquartile distributions of variables**

Country	Sample		CDS		Global financial var.				Macroeconomic sentiment var.								Political and Geop. var.			
					FED		VIX		ECO		INT		EPU		TPU		GPR		POL	
	Start	End	p25	p75	p25	p75	p25	p75	p25	p75	p25	p75	p25	p75	p25	p75	p25	p75	p25	p75
Argentina	11/08/2020	13/06/2025	-0.78	0.77	-1.30	0.79	-0.72	0.60	-0.72	0.77	-0.39	0.68	-0.68	0.29	-0.77	0.66	-0.82	0.70	-0.76	0.52
Australia	01/01/2018	13/06/2025	-0.64	0.66	-1.03	0.99	-0.71	0.41	-0.34	0.61	-0.49	0.70	-0.65	0.30	-0.63	0.41	-0.69	0.58	-0.72	0.58
Austria	01/01/2018	13/06/2025	-0.95	0.64	-1.03	0.99	-0.71	0.41	-0.39	0.61	-0.39	0.66	-0.64	0.27	-0.56	0.21	-0.57	0.33	-0.69	0.61
Belgium	01/01/2018	13/06/2025	-0.82	0.63	-1.03	0.99	-0.71	0.41	-0.34	0.64	-0.36	0.67	-0.69	0.48	-0.71	0.53	-0.58	0.44	-0.67	0.45
Brazil	01/01/2018	13/06/2025	-0.73	0.66	-1.03	0.99	-0.71	0.41	-0.37	0.67	-0.38	0.67	-0.76	0.57	-0.76	0.52	-0.70	0.57	-0.72	0.47
Canada	21/02/2019	14/06/2025	-0.82	0.78	-1.19	0.96	-0.68	0.44	-0.41	0.68	-0.36	0.68	-0.54	0.16	-0.44	-0.05	-0.72	0.61	-0.75	0.57
Chile	01/01/2018	13/06/2025	-0.65	0.43	-1.03	0.99	-0.71	0.41	-0.62	0.72	-0.52	0.55	-0.73	0.54	-0.69	0.60	-0.67	0.54	-0.85	0.61
China	01/01/2018	13/06/2025	-0.79	0.57	-1.03	0.99	-0.71	0.41	-0.73	0.79	-0.50	0.76	-0.64	0.37	-0.58	0.45	-0.75	0.58	-0.55	0.52
Colombia	01/01/2018	13/06/2025	-0.91	0.67	-1.03	0.99	-0.71	0.41	-0.29	0.58	-0.21	0.50	-0.75	0.54	-0.67	0.52	-0.69	0.49	-0.74	0.66
CzechRep	01/01/2018	13/06/2025	-0.78	0.80	-1.03	0.99	-0.71	0.41	-0.45	0.54	-0.04	0.34	-0.68	0.45	-0.69	0.69	-0.70	0.44	-0.68	0.57
Denmark	01/01/2018	13/06/2025	-0.74	0.49	-1.03	0.99	-0.71	0.41	-0.50	0.71	-0.29	0.60	-0.72	0.46	-0.70	0.51	-0.64	0.45	-0.62	0.41
Egypt	01/01/2018	13/06/2025	-0.74	0.30	-1.03	0.99	-0.71	0.41	-0.44	0.56	-0.33	0.51	-0.68	0.54	-0.67	0.58	-0.75	0.49	-0.66	0.47
Finland	01/01/2018	13/06/2025	-0.79	0.80	-1.03	0.99	-0.71	0.41	-0.46	0.69	-0.57	0.73	-0.68	0.47	-0.70	0.49	-0.70	0.48	-0.58	0.51
France	01/01/2018	13/06/2025	-0.78	0.55	-1.03	0.99	-0.71	0.41	-0.29	0.60	-0.36	0.61	-0.49	0.10	-0.67	0.47	-0.60	0.44	-0.79	0.59
Germany	01/01/2018	13/06/2025	-0.69	0.34	-1.03	0.99	-0.71	0.41	-0.41	0.66	-0.38	0.66	-0.67	0.36	-0.72	0.58	-0.61	0.40	-0.69	0.59
Hungary	01/01/2018	13/06/2025	-0.75	0.52	-1.03	0.99	-0.71	0.41	-0.50	0.64	-0.15	0.56	-0.69	0.55	-0.71	0.48	-0.57	0.31	-0.60	0.49
India	01/01/2018	13/06/2025	-0.59	0.47	-1.03	0.99	-0.71	0.41	-0.46	0.63	-0.42	0.71	-0.67	0.38	-0.69	0.47	-0.66	0.46	-0.75	0.59
Indonesia	01/01/2018	13/06/2025	-0.72	0.42	-1.03	0.99	-0.71	0.41	-0.64	0.63	-0.28	0.62	-0.62	0.25	-0.61	0.38	-0.66	0.58	-0.67	0.60
Israel	01/01/2018	13/06/2025	-0.75	0.17	-1.03	0.99	-0.71	0.41	-0.49	0.74	-0.38	0.70	-0.69	0.51	-0.52	-0.06	-0.74	0.57	-0.86	0.59
Italy	01/01/2018	13/06/2025	-0.83	0.58	-1.03	0.99	-0.71	0.41	-0.43	0.74	-0.17	0.61	-0.79	0.58	-0.54	0.09	-0.62	0.44	-0.63	0.37
Japan	01/01/2018	13/06/2025	-0.71	0.47	-1.03	0.99	-0.71	0.41	-0.42	0.68	-0.40	0.68	-0.75	0.58	-0.75	0.45	-0.73	0.52	-0.70	0.38
Jordan	27/10/2023	13/06/2025	-0.63	0.55	-0.83	0.87	-0.76	0.41	-0.64	0.49	-0.36	0.64	-0.65	0.26	-0.73	0.65	-0.78	0.59	-0.63	0.63
Malaysia	01/01/2018	13/06/2025	-0.78	0.57	-1.03	0.99	-0.71	0.41	-0.66	0.63	-0.43	0.66	-0.66	0.30	-0.72	0.55	-0.84	0.69	-0.68	0.68
Mexico	01/01/2018	13/06/2025	-0.66	0.34	-1.03	0.99	-0.71	0.41	-0.35	0.64	-0.27	0.60	-0.72	0.66	-0.59	0.19	-0.69	0.58	-0.64	0.53
Morocco	01/01/2018	13/06/2025	-0.56	0.17	-1.03	0.99	-0.71	0.41	-0.56	0.52	-0.16	0.42	-0.74	0.61	-0.69	0.62	-0.68	0.52	-0.66	0.58
Netherlands	01/01/2018	13/06/2025	-0.79	0.35	-1.03	0.99	-0.71	0.41	-0.70	0.72	-0.32	0.64	-0.74	0.51	-0.74	0.52	-0.64	0.49	-0.67	0.43
Norway	01/01/2018	13/06/2025	-0.71	0.44	-1.03	0.99	-0.71	0.41	-0.45	0.73	-0.27	0.62	-0.70	0.38	-0.63	0.14	-0.65	0.57	-0.80	0.66
Peru	01/01/2018	13/06/2025	-0.53	0.37	-1.03	0.99	-0.71	0.41	-0.39	0.60	-0.31	0.62	-0.59	0.22	-0.64	0.45	-0.60	0.43	-0.64	0.36
Philippines	01/01/2018	13/06/2025	-0.78	0.69	-1.03	0.99	-0.71	0.41	-0.52	0.75	-0.20	0.54	-0.61	0.35	-0.71	0.51	-0.76	0.68	-0.69	0.45
Poland	01/01/2018	13/06/2025	-0.52	0.00	-1.03	0.99	-0.71	0.41	-0.45	0.69	-0.37	0.65	-0.74	0.51	-0.64	0.40	-0.71	0.50	-0.73	0.67
Qatar	01/01/2018	13/06/2025	-0.65	0.49	-1.03	0.99	-0.71	0.41	-0.65	0.49	-0.12	0.47	-0.64	0.25	-0.68	0.46	-0.75	0.36	-0.54	0.40
Russia	01/01/2018	06/04/2022	-0.21	-0.11	-1.08	1.02	-0.67	0.36	-0.15	0.61	0.01	0.48	-0.76	0.51	-0.67	0.45	-0.50	0.36	-0.62	0.30
SaudiA.	01/01/2018	13/06/2025	-0.65	0.46	-1.03	0.99	-0.71	0.41	-0.42	0.56	-0.14	0.55	-0.76	0.53	-0.73	0.55	-0.73	0.57	-0.55	0.44
Spain	01/01/2018	13/06/2025	-0.76	0.38	-1.03	0.99	-0.71	0.41	-0.35	0.65	-0.27	0.58	-0.65	0.39	-0.52	0.27	-0.63	0.41	-0.67	0.51
Sweden	01/01/2018	13/06/2025	-0.71	0.83	-1.03	0.99	-0.71	0.41	-0.53	0.69	-0.41	0.68	-0.71	0.45	-0.45	0.11	-0.64	0.52	-0.76	0.60
Thailand	01/01/2018	13/06/2025	-0.55	0.31	-1.03	0.99	-0.71	0.41	-0.44	0.72	-0.25	0.50	-0.60	0.36	-0.42	0.19	-0.68	0.43	-0.28	0.59
Turkey	01/01/2018	13/06/2025	-0.77	0.73	-1.03	0.99	-0.71	0.41	-0.46	0.64	-0.20	0.53	-0.66	0.47	-0.68	0.50	-0.74	0.59	-0.47	0.56
UK	01/01/2018	13/06/2025	-0.71	0.72	-1.03	0.99	-0.71	0.41	-0.39	0.69	-0.43	0.69	-0.65	0.44	-0.55	0.34	-0.62	0.39	-0.66	0.41
USA	01/01/2018	13/06/2025	-0.79	0.76	-1.03	0.99	-0.71	0.41	-0.17	0.58	-0.45	0.70	-0.62	0.28	-0.69	0.41	-0.63	0.50	-0.72	0.51
Ukraine	17/01/2020	06/04/2022	-0.33	-0.14	-0.54	0.09	-0.73	0.28	-0.41	0.70	0.15	0.47	-0.81	0.59	-0.72	0.47	-0.69	0.29	-0.67	0.67
Uruguay	01/01/2018	13/06/2025	-0.75	0.45	-1.03	0.99	-0.71	0.41	-0.49	0.65	-0.48	0.69	-0.71	0.51	-0.62	0.59	-0.72	0.54	-0.79	0.65
Vietnam	01/01/2018	13/06/2025	-0.69	0.40	-1.03	0.99	-0.71	0.41	-0.70	0.64	-0.60	0.66	-0.68	0.35	-0.65	0.26	-0.78	0.75	-0.23	0.56

Notes: The table reports country-specific sample periods and interquartile ranges (25th and 75th percentiles) for all variables used in the empirical analysis. The sample covers 42 sovereigns over January 2018–July 2025 (unbalanced panel); start dates vary by CDS data availability. All variables are expressed as 28-day moving averages, demeaned and standardized to zero mean and unit variance within each country. **CDS**: 5-year sovereign credit default swap spread (basis points, standardized). **Global financial variables**: FED = 2-year U.S. Treasury yield (proxy for global monetary policy); VIX = CBOE Volatility Index (proxy for global financial volatility). **Macroeconomic sentiment variables**: ECO = local economic sentiment index; INT = local interest-rate sentiment index; EPU = Economic Policy Uncertainty index; TPU = Trade Policy Uncertainty index. **Political and geopolitical variables**: GPR = Geopolitical Risk index; POL = Political Tensions index. All news-based indicators (ECO, INT, EPU, TPU, GPR, POL) are constructed by BBVA Research from GDELT data as described in Appendix A.2. FED and VIX are global (non-country-specific) variables; their interquartile ranges differ across countries only because of variation in sample periods. Russia and Ukraine have truncated samples ending in June 2022 and January 2020, respectively, reflecting CDS market disruptions following the onset of the conflict. Jordan enters the sample in October 2023.

A.2 Media sentiment indicators development process

All news-based indicators are constructed by BBVA Research using the Global Database of Events, Language, and Tone (Leetaru and Schrodt, 2013). Each index is computed at the country–day level, smoothed with a 28-day moving average, and standardized to zero mean and unit variance over the country-specific sample period. No outlier treatment is applied, as extreme events are informative signals of shifts in risk perception. Four indices are used.[23]

Economic Policy Uncertainty (EPU). Following Baker et al. (2016), the EPU index measures the relative coverage of news articles that jointly mention a country name, terms related to economic uncertainty, and policy-relevant institutions or instruments. The generic query template is:

```
{COUNTRY_NAME} (uncertain OR uncertainty) (economic OR economy) (policy OR tax OR
spending OR regulation OR central bank OR budget OR deficit)
```

Country-specific queries adapt this template to local institutional vocabulary. For instance, the United States query adds references to Congress, the White House, and the Federal Reserve; Mexico includes Banxico, BdeM, and the Chamber of Deputies; Spain references Hacienda, parliament, and specific fiscal terms.[24] The index equals the ratio of EPU-related articles to total published articles for each country–day.

Trade Policy Uncertainty (TPU). Following Caldara et al. (2020), the TPU index captures news coverage related to trade-policy instruments. The query requires the co-occurrence of a trade term and a policy-instrument term:

```
(tariff OR tariffs OR import OR imports OR export OR exports OR trade OR dumping OR
antidumping OR GATT OR WTO) (duty OR duties OR barrier OR barriers OR ban OR bans OR
tax OR taxes OR subsidy OR subsidies)
```

The index equals the ratio of TPU-related articles to total published articles. Unlike the EPU, the TPU query is uniform across countries.

Geopolitical Risk (GPR). Following Caldara and Iacoviello (2022), the GPR index combines tone (sentiment) and relative coverage of articles classified under two groups of GDELT conflict-related taxonomy themes. Group 1 covers military and political-violence categories (e.g., `WAR`, `CONFLICT`, `TERROR`, `MILITARY`, `REBELLION`, `PEACEKEEPING`). Group 2 covers threat and disruption categories (e.g., `SANCTIONS`, `BLOCKADE`, `ARMEDCONFLICT`, `CRISIS`, `RAID`, `KILL`). An article must match at least one theme from each group. The index is the product of tone and relative coverage, multiplied by -1 for interpretability (higher values = greater geopolitical risk).

Political Tensions (POL). The Political Tensions Index captures tone and coverage of news classified under the GDELT taxonomy theme `USPEC_POLITICS_GENERAL1` (elections, government institutions, legislative activity, political scandals, civil rights, national security, among others) that additionally contain at least one of the following keywords: *political instability, political uncertainty, political crisis, political polarization, political extremism, political turmoil, political conflict*. As with GPR, the index is the product of tone and relative coverage, multiplied by -1.

[23] Complete country-specific keyword lists and GDELT taxonomy codes for all 42 countries are available in the replication package at `https://bigdata.bbvaresearch.com/en/`.

[24] Representative examples: *United States*: "United States (uncertainty OR uncertain) (economic OR economy) (congress OR legislation OR white house OR regulation OR federal reserve OR deficit)"; *Mexico*: "Mexico (economic OR economy) (uncertain OR uncertainty) (regulation OR deficit OR budget OR Bank OR BdeM OR Banxico OR congress OR senate OR deputies OR legislation OR taxes OR Federal Reserve)"; *Spain*: "Spain (uncertainty OR uncertain OR instability OR risk) (economic OR economy) (parliament OR government OR Hacienda OR deficit OR budget OR expenditure OR debt OR taxes OR law OR reform OR regulation OR Bank)".

Figure 7: Unconditional Associations between News Indicators and Sovereign Spreads by Region

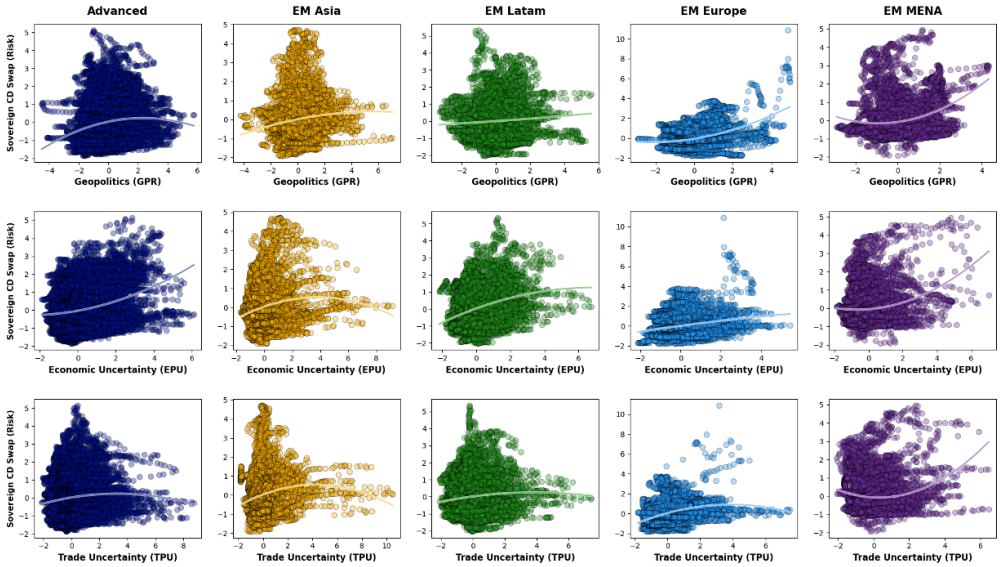

Notes: Each panel plots a LOESS-smoothed relationship between a news-based indicator and sovereign CDS spreads, segmented by asset class and EM region. Rows: GPR, EPU, TPU. Columns: Advanced, EM Asia, EM Latam, EM Europe, EM MENA. Scatter points exclude extreme tails.

B Appendix B. Shapley Dependence and Interaction Analysis

Figure 8: **Interaction Strength among Sovereign Risk Drivers across Countries**

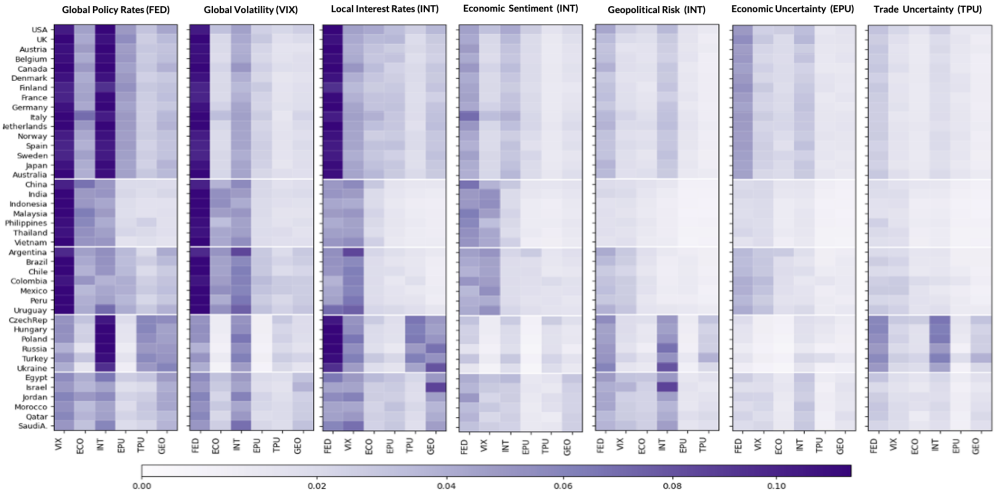

Notes: Heatmaps of pairwise Shapley–Taylor interaction intensities between each core driver and all other variables at the country level. Rows represent countries ordered by region; columns represent remaining variables. Darker shading indicates larger absolute interaction values. The dominant interactions involve US2Y×VIX and US2Y×INT, confirming that global financial conditions govern the strength of higher-order complementarities. GPR and EPU interactions are weak for Advanced Economies but markedly stronger in EM Europe and MENA. See Section 4.3 for discussion.

C Appendix C. Spillover and Network Interconnectedness

We apply two interconnectedness measures to the panel of daily, country-level Shapley attributions — computed from SHAP values rather than raw CDS spreads, which allows tracking interconnectedness *within* each risk channel separately.

Panel construction. Let $s_{i,t}^{(f)}$ denote the SHAP-implied contribution of feature f to the CDS spread of country i on date t. For each feature and evaluation date t_0 (weekly from January 2021), we extract a rolling window of 60–180 days. Countries observed on fewer than 70% of days are dropped; the ten with highest coverage and variance are retained to avoid over-parameterized VARs.

Diebold–Yilmaz spillover index. A VAR(p) with $p^* \in \{1, 2, 3, 4\}$ chosen by AIC is estimated on each window. Following Pesaran and Shin (1998) and Diebold and Yilmaz (2014), the generalized H-step forecast-error variance share of country j in country i is:

$$\theta_{ij}(H) = \frac{\sum_{\ell=0}^{H-1} \left(e_i' \Psi_\ell \Sigma_u^\lambda e_j\right)^2}{\sum_{\ell=0}^{H-1} \left(e_i' \Psi_\ell \Sigma_u^\lambda \Psi_\ell' e_i\right)},$$

with rows normalized to sum to unity. The total spillover index is $S^{\text{DY}}(H) = 100 \cdot \sum_{i \neq j} \tilde{\theta}_{ij}(H) \,/\, k$.

Network density. As a complementary non-parametric measure, we compute the weighted density of the Spearman rank-correlation network, retaining edges with $|\rho_{ij}| \geq 0.40$:

$$\text{Density Index} = 100 \cdot \frac{\sum_{i<j} |\rho_{ij}| \cdot \mathbf{1}\{|\rho_{ij}| \geq \tau\}}{k(k-1)/2}.$$

High spillovers with high density correspond to systemic stress; high density with low spillovers indicates common-shock repricing without durable contagion.

Diebold-Yilmaz Interconnectedness and Network Density graph

Figure 9 displays both indices—the DY total spillover (blue) and weighted network density (orange)—from 2021 onward, with vertical markers for the Russia–Ukraine invasion (February 2022), the Hamas–Israel conflict (October 2023), and the 2024 U.S. election. Equalized vertical scales permit direct comparison across variables.

Figure 9: **Cross-Country Connectedness of Sovereign Risk Drivers, 2021–2025**

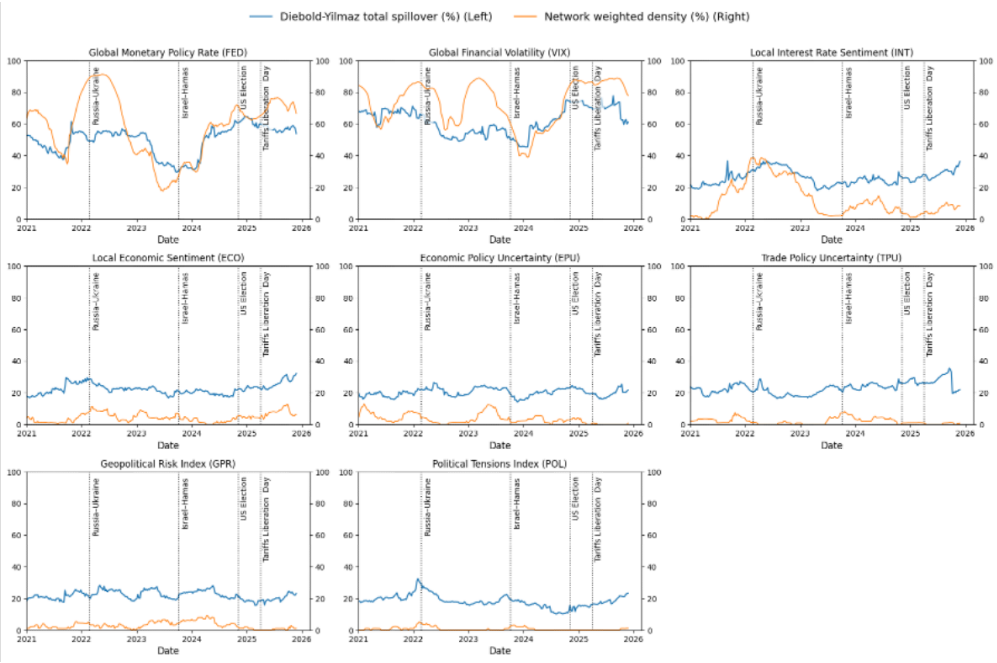

Notes: The figure reports dynamic spillover effects (blue line) and network density (orange line) for sovereign-risk determinants. Top row: global financial drivers (2-year UST, VIX, local interest rate sentiment). Middle row: local economic sentiment and uncertainty indices (EPU, TPU). Bottom row: geopolitical risk (GPR) and political tensions (POL). All indices are computed from daily, country-level Shapley attributions.

D Appendix D. Country-Level Transmission Dynamics

Figure 10: **Russia–Ukraine Invasion: Country-Level Shapley Dynamics**

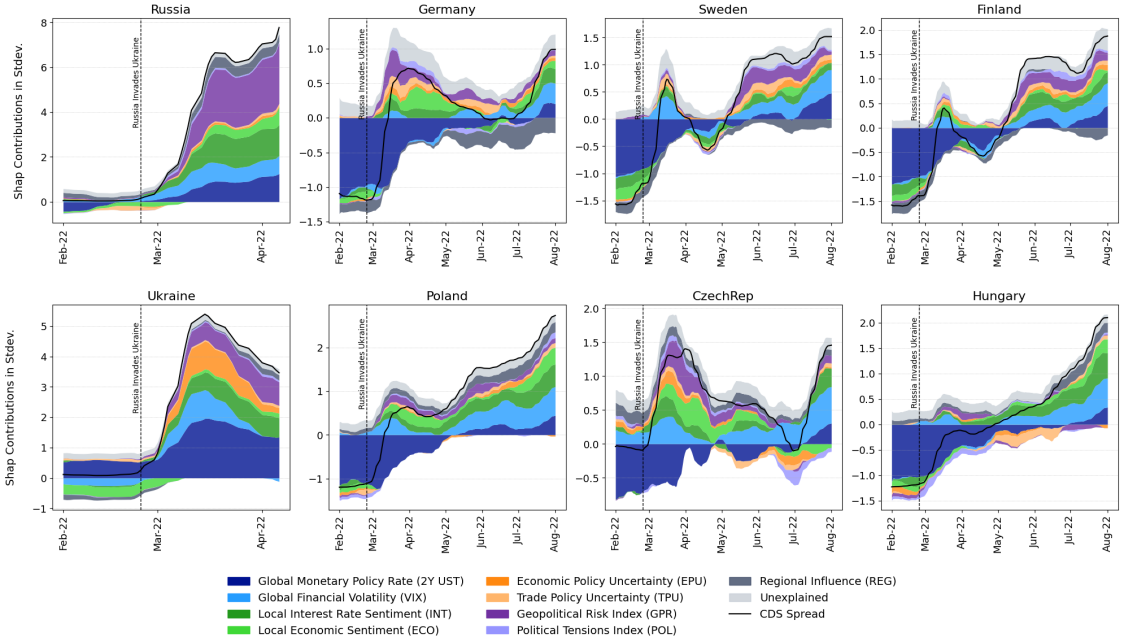

Notes: Each panel plots the evolution of Shapley contributions to sovereign CDS spreads for selected countries before and after February 2022. Stacked areas represent individual predictor contributions; black line is the observed CDS spread. For Russia and Ukraine, contributions from GPR, global financial volatility, and domestic conditions surge simultaneously. For European economies, the initial geopolitical impulse is followed by a cascade through domestic inflation, local rate tightening, and global financial tightening. All series are 28-day moving averages.

Figure 11: **Hamas–Israel Conflict: Country-Level Shapley Dynamics**

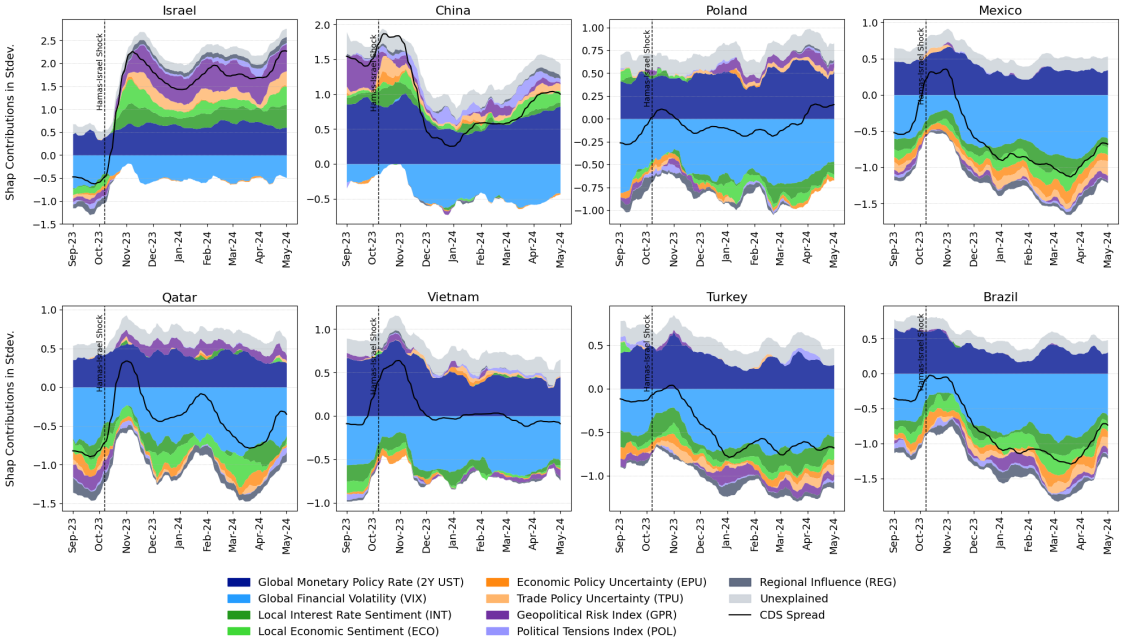

Notes: The figure plots the evolution of Shapley contributions to sovereign CDS spreads for selected countries before and after October 2023. For Israel, GPR and domestic condition contributions surge. For neighboring economies (Qatar, Turkey), increases are muted. For most other emerging markets and Asian economies, geopolitical contributions remain essentially flat, underscoring the contained nature of the shock.

Figure 12: **U.S. Presidential Election (Nov. 2024) and Liberation Day Tariffs (Apr. 2025): Country-Level Shapley Dynamics**

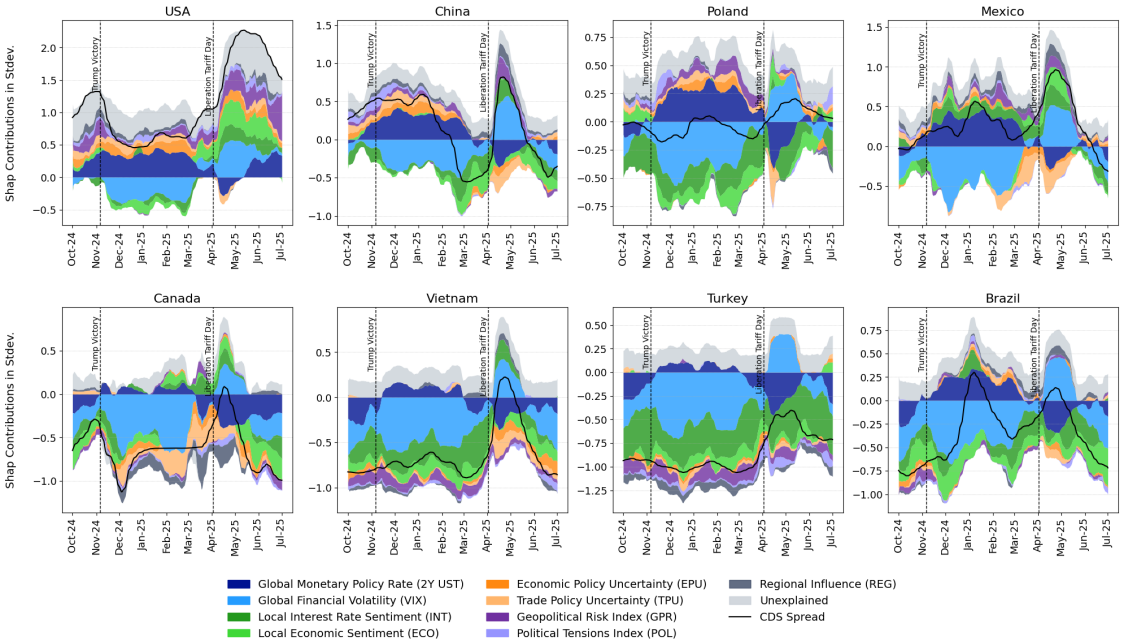

Notes: The figure shows Shapley contribution dynamics around the 2024 U.S. election and subsequent tariff announcements. For the United States, sovereign risk increases after the election and accelerates with tariff measures, driven by TPU, EPU, and global volatility. Spillovers are evident in Mexico, Canada, China, and Brazil through trade and policy uncertainty. For other economies, global financial drivers remain central, with uncertainty effects rising around tariff dates.

Figure 13: **Gravity Validation: Direct Channel vs. Regional Component — Russia–Ukraine (Feb. 2022)**

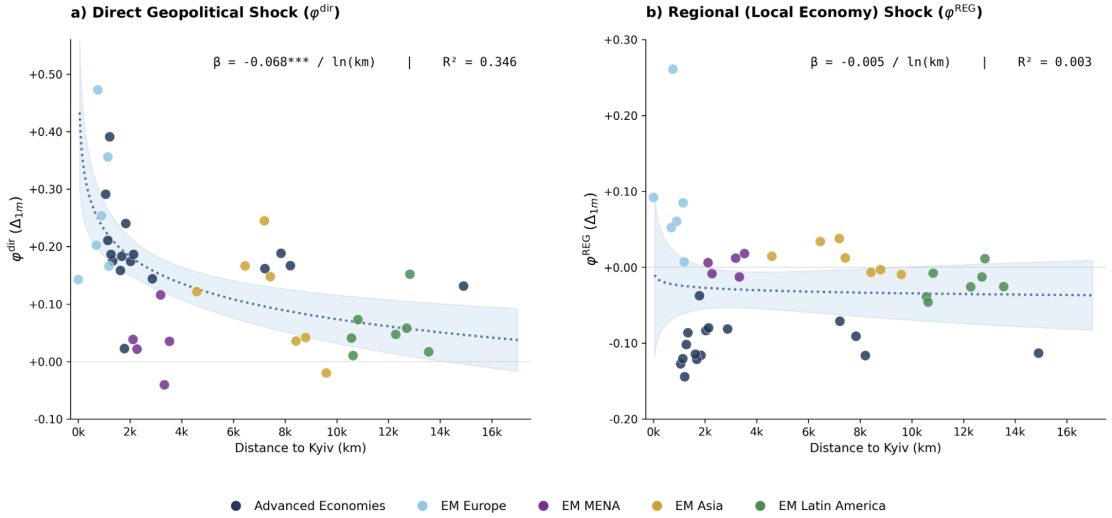

Notes: Panel (a) plots the one-month Direct-channel response $\varphi_i^{\text{dir}}(\Delta_{1m})$ and panel (b) the REG-within-LOC Shapley value $\varphi_i^{\text{REG}}(\Delta_{1m})$ against geodesic distance from each country's capital to Kyiv. The Direct channel exhibits significant gravity-like decay ($\hat{\beta} = -0.068^{***}$, $R^2 = 0.346$), consistent with geopolitical shocks repricing default risk in proportion to conflict proximity. The regional component—which captures the Shapley–Taylor attribution of the regional group indicators (Advanced, EM Europe, EM MENA, EM Asia, EM Latin America) absorbed into the Local channel—shows no distance relationship ($\hat{\beta} = -0.005$, $R^2 = 0.003$, $p = 0.72$), confirming that it does not proxy for geographic proximity. This contrast validates the absorption of REG into the Local channel rather than the creation of a fifth transmission channel. Dotted lines: OLS log-distance fit from eq. (7); shaded bands: 95% confidence intervals. $^{***}\, p < 0.01$, $^{**}\, p < 0.05$, $^{*}\, p < 0.10$. OLS includes all countries with available CDS data (excluding Ukraine at $d = 0$).

E Appendix E. Country-Level Channel Decomposition Tables

Tables 6 and 7 report the four-channel Shapley–Taylor decomposition at the country level for each of the four episodes analysed in Section 5. Each cell shows $\Delta_{1m} \equiv \bar{\varphi}^{post}_{1m} - \bar{\varphi}^{pre}$, the short-term change in the channel contribution (in σ-CDS units) between the three-month pre-event window and the one-month post-event window.[25]

Table 6: **Geopolitical Episodes** — Country-level channel decomposition (Δ_{1m})

	Russia–Ukraine (Feb. 2022)					Hamas–Israel (Oct. 2023)				
Country	φ^{dir}	φ^{GFC}	φ^{UNC}	φ^{LOC}	φ^{tot}	φ^{dir}	φ^{GFC}	φ^{UNC}	φ^{LOC}	φ^{tot}
Advanced Economies										
Group avg.	+.18	−.16	.00	−.17	−.15	+.10	−.03	.00	−.07	−.01
USA	+.18	−.14	+.01	−.17	−.12	+.11	−.15	−.05	−.09	−.18
Canada	+.14	−.10	+.02	−.20	−.14	+.13	−.07	−.01	−.12	−.08
Australia	+.10	−.17	+.02	−.20	−.25	+.11	−.18	−.03	−.11	−.21
UK	+.19	−.15	+.01	−.19	−.14	+.13	+.04	+.01	−.09	+.09
Germany	+.36	−.32	+.03	−.03	+.03	+.12	−.15	−.02	−.02	−.06
France	+.18	−.10	+.01	−.17	−.07	+.17	−.06	−.04	−.11	−.04
Italy	+.16	−.31	+.02	−.36	−.49	+.14	−.02	−.06	−.14	−.07
Spain	+.14	−.13	+.01	−.11	−.09	+.15	−.07	−.02	−.14	−.07
Netherlands	+.05	−.08	−.01	−.15	−.18	+.04	+.07	+.02	+.01	+.14
Belgium	+.22	−.20	−.01	−.15	−.14	+.15	−.01	+.02	−.14	+.02
Austria	+.29	−.28	.00	−.09	−.08	+.12	−.12	.00	−.06	−.06
Denmark	+.17	−.11	−.02	−.11	−.07	.00	+.03	+.01	+.02	+.07
Finland	+.22	−.13	−.02	−.23	−.16	+.08	+.03	+.02	−.03	+.10
Norway	+.16	−.14	−.03	−.18	−.19	+.07	+.08	+.02	−.06	+.11
Sweden	+.17	−.09	.00	−.22	−.14	+.02	+.07	+.04	−.04	+.09
Japan	+.15	−.13	+.01	−.23	−.20	+.06	+.03	−.01	−.01	+.08
Emerging Europe										
Group avg.	+.24	+.06	+.05	+.36	+.71	+.07	−.03	−.01	−.03	.00
Russia	+.41	+.89	+.25	+1.46	+3.01	—	—	—	—	—
Ukraine	+.10	+.42	+.03	+.43	+.98	—	—	—	—	—
Poland	+.19	−.17	+.03	+.11	+.15	−.02	.00	−.01	−.03	−.06
Czech Rep.	+.35	−.35	+.02	+.15	+.18	+.06	+.03	.00	+.02	+.11
Hungary	+.24	−.25	.00	+.04	+.03	+.11	−.04	.00	−.05	+.02
Turkey	+.14	−.19	−.01	−.04	−.09	+.13	−.10	−.02	−.07	−.07
Middle East & North Africa										
Group avg.	+.03	−.07	−.01	−.11	−.16	+.19	+.07	+.03	+.18	+.47
Egypt	−.02	−.04	−.02	−.17	−.25	+.33	+.13	+.02	+.37	+.85
Israel	+.05	−.01	−.01	−.07	−.04	+.20	+.13	+.09	+.38	+.80
Morocco	+.06	−.14	−.02	−.07	−.16	+.04	+.08	.00	−.01	+.11
Qatar	−.04	−.07	.00	−.13	−.24	+.18	+.07	+.02	+.04	+.31
Saudi Arabia	+.12	−.11	−.01	−.10	−.10	+.18	−.06	+.01	+.13	+.26
Asia-Pacific										
Group avg.	+.09	−.15	−.01	−.01	−.07	+.07	−.08	.00	−.08	−.09
China	+.13	−.20	−.01	+.03	−.06	+.01	−.41	−.04	−.17	−.61
India	+.14	−.16	.00	−.03	−.05	−.03	−.07	−.01	−.03	−.13
Indonesia	−.06	+.02	+.02	−.04	−.06	+.11	.00	+.01	−.08	+.04
Malaysia	.00	−.09	.00	−.09	−.18	+.01	−.07	.00	−.03	−.08
Philippines	+.03	−.09	+.01	−.04	−.09	+.17	−.06	+.01	−.17	−.05
Thailand	+.15	−.15	−.02	+.06	+.04	+.12	+.13	+.02	−.02	+.25
Vietnam	+.24	−.34	−.05	+.07	−.08	+.10	−.08	+.03	−.09	−.03
Latin America										
Group avg.	+.04	−.11	−.02	−.05	−.14	+.02	.00	−.01	−.01	.00
Argentina	+.13	−.13	−.03	−.05	−.09	+.03	.00	−.01	−.03	.00
Brazil	+.01	−.16	−.03	−.11	−.29	+.01	.00	−.03	.00	−.03
Chile	.00	−.05	−.01	−.05	−.10	+.01	+.04	+.01	−.01	+.05
Colombia	+.01	−.13	−.04	−.05	−.21	+.01	+.01	−.01	−.06	−.05
Mexico	+.03	−.08	+.02	−.13	−.15	+.05	−.09	.00	.00	−.04
Peru	+.05	−.11	−.02	.00	−.07	+.07	+.01	−.01	+.01	+.08
Uruguay	+.03	−.10	−.02	+.02	−.07	−.05	+.04	.00	.00	−.01

$\Delta > +0.05$ $+0.005 < \Delta \leq +0.05$ $|\Delta| \leq 0.005$ $-0.05 \leq \Delta < -0.005$ $\Delta < -0.05$. Russia/Ukraine excl. from Hamas–Israel (no pre-event data). φ^{LOC} includes Region cross-SHAP.

[25] Persistence results (Δ_{3m}) are qualitatively similar and available from the authors upon request.

Table 7: **Geoeconomic Episodes** — Country-level channel decomposition (Δ_{1m})

	Trump Election (Nov. 2024)					Liberation Day (Apr. 2025)				
Country	φ^{dir}	φ^{GFC}	φ^{UNC}	φ^{LOC}	φ^{tot}	φ^{dir}	φ^{GFC}	φ^{UNC}	φ^{LOC}	φ^{tot}
USMCA										
Group avg.	+.04	−.08	+.01	+.02	−.01	—	—	—	—	—
USA	+.04	−.08	+.01	+.05	+.03	.00	−.09	−.04	+.03	−.10
Canada	+.04	−.12	−.02	+.01	−.08	.00	+.08	+.04	+.21	+.33
Mexico	+.03	−.04	+.02	+.01	+.02	+.01	−.04	+.07	+.04	+.08
Advanced Economies										
Group avg.	+.04	−.07	+.04	+.04	+.04	−.02	−.13	−.02	.00	−.17
Australia	+.04	−.13	+.05	+.03	−.01	−.03	−.14	−.05	+.04	−.18
UK	+.04	−.06	+.03	+.02	+.03	−.01	−.13	−.03	.00	−.17
Germany	+.04	−.04	+.05	+.07	+.12	−.01	−.12	+.01	−.01	−.13
France	+.03	+.08	+.04	+.09	+.23	−.01	−.05	+.01	+.04	−.02
Italy	+.04	−.15	+.06	−.03	−.09	−.02	−.24	−.01	−.07	−.33
Spain	+.03	−.13	+.01	+.03	−.07	−.02	−.12	−.02	+.01	−.14
Netherlands	+.05	−.12	+.06	+.03	+.02	−.02	−.06	−.02	−.01	−.10
Japan	+.02	−.02	+.04	+.06	+.10	−.02	−.18	−.06	.00	−.26
Emerging Europe										
Group avg.	+.04	−.06	+.02	−.01	−.01	−.02	−.03	.00	+.02	−.03
Poland	+.03	−.03	+.02	.00	+.02	−.02	−.07	−.01	−.04	−.13
Czech Rep.	+.04	−.07	+.05	+.01	+.02	−.01	−.03	+.02	−.04	−.06
Hungary	+.04	−.09	+.01	−.01	−.04	−.03	−.01	−.01	+.12	+.07
Turkey	+.04	−.05	.00	−.03	−.04	−.02	−.02	.00	+.02	−.01
Asia-Pacific										
Group avg.	+.02	−.07	+.03	+.03	+.02	−.03	−.13	−.02	.00	−.17
China	+.03	−.04	+.05	+.06	+.10	.00	−.14	−.03	−.08	−.26
India	+.03	−.12	.00	+.03	−.06	−.02	−.20	−.04	−.07	−.33
Indonesia	+.03	−.08	+.02	+.03	.00	−.02	−.10	−.03	+.01	−.14
Malaysia	.00	−.05	+.02	+.01	−.01	−.04	−.15	−.05	+.07	−.16
Philippines	+.03	−.10	+.03	.00	−.04	−.04	−.03	.00	+.04	−.02
Thailand	+.02	−.02	+.06	+.04	+.10	−.05	−.07	−.02	+.06	−.08
Vietnam	+.03	−.06	+.03	+.03	+.03	−.02	−.21	.00	+.01	−.22
Latin America										
Group avg.	+.03	−.07	+.04	+.01	+.01	−.02	−.07	+.02	−.01	−.08
Argentina	+.03	−.04	+.05	−.04	−.01	−.02	−.11	−.01	−.05	−.19
Brazil	+.05	−.11	+.06	+.05	+.05	.00	−.10	−.01	−.06	−.16
Chile	+.02	−.06	+.05	+.02	+.03	−.04	−.02	+.02	+.01	−.03
Colombia	+.01	−.07	+.02	+.03	−.01	−.01	−.07	+.03	−.02	−.06
Peru	+.05	−.07	+.06	−.01	+.03	−.02	−.03	+.05	+.02	+.01
Uruguay	−.01	−.06	+.03	+.01	−.03	−.02	−.06	+.03	.00	−.05
Middle East & North Africa										
Group avg.	+.02	−.06	+.03	+.01	+.01	−.02	−.05	+.02	+.01	−.05
Egypt	+.01	−.06	+.01	+.02	−.02	−.01	−.09	+.03	−.05	−.11
Israel	+.03	−.05	+.02	−.03	−.03	−.02	−.02	.00	+.01	−.02
Qatar	+.01	−.11	+.04	+.03	−.02	−.03	−.06	.00	.00	−.09
Saudi Arabia	+.04	−.04	+.06	+.03	+.09	−.03	−.04	+.04	+.06	+.03

$\Delta > +0.05$ $+0.005 < \Delta \leq +0.05$ $|\Delta| \leq 0.005$ $-0.05 \leq \Delta < -0.005$ $\Delta < -0.05$. Liberation Day USMCA group avg. not reported separately; see individual countries. φ^{LOC} includes Region cross-SHAP.

F Appendix F. Local Projection Robustness

Table 8: Average Innovation LP : Estimated Channel Impulse Responses at $h = 5$, 30, and 60 Days

Event	Channel	$h = 5$		$h = 30$		$h = 60$	
		$\hat{\beta}$	Sig.	$\hat{\beta}$	Sig.	$\hat{\beta}$	Sig.
Russia–Ukraine GPR, Feb. 2022 *Geopolitical*	φ^{dir}	0.0130	–	0.0050	–	0.0034	–
	φ^{GFC}	-0.0039	–	-0.0007	–	-0.0002	–
	φ^{UNC}	-0.0012	–	-0.0003	–	-0.0002	–
	φ^{LOC}	-0.0077	–	-0.0037	–	-0.0023	–
Hamas–Israel GPR, Oct. 2023 *Geopolitical*	φ^{dir}	0.0130	–	0.0050	–	0.0034	–
	φ^{GFC}	-0.0039	–	-0.0007	–	-0.0002	–
	φ^{UNC}	-0.0012	–	-0.0003	–	-0.0002	–
	φ^{LOC}	-0.0077	–	-0.0037	–	-0.0023	–
U.S. Election EPU, Nov. 2024 *Geoeconomic*	φ^{dir}	0.0034	–	0.0017	–	0.0014	–
	φ^{GFC}	0.0032	–	0.0017	–	0.0010	–
	φ^{UNC}	0.0008	–	0.0006	–	0.0004	–
	φ^{LOC}	-0.0006	–	0.0003	–	0.0003	–
"Liberation Day" TPU, Apr. 2025 *Geoeconomic*	φ^{dir}	-0.0020	–	-0.0008	–	-0.0005	–
	φ^{GFC}	-0.0016	–	-0.0010	–	-0.0000	–
	φ^{UNC}	0.0015	–	0.0009	–	0.0005	–
	φ^{LOC}	-0.0009	–	0.0000	–	0.0002	–

Notes: Estimated impulse responses from panel local projections (Jordà, 2005) using AR(5) residual innovations as structural shocks. Standard errors follow Driscoll and Kraay (1998) with bandwidth $= \max(20,\ h)$, with country and time fixed effects and 5 lags of Δy. Contemporaneous controls: global VIX (moving average) and sovereign yield spread (moving average).

Table 9: Narrative LP: Estimated Channel Impulse Responses at $h = 5$, 30, and 60 Days

Event	Channel	$h = 5$		$h = 30$		$h = 60$	
		$\hat{\beta}$	Sig.	$\hat{\beta}$	Sig.	$\hat{\beta}$	Sig.
Russia–Ukraine GPR, Feb. 2022 *Geopolitical*	φ^{dir}	0.1031	***	0.1213	***	0.0948	***
	φ^{GFC}	-0.0782	***	-0.1035	***	-0.0808	***
	φ^{UNC}	-0.0110	***	-0.0096	*	-0.0013	–
	φ^{LOC}	-0.0728	***	-0.0234	–	-0.0540	***
Hamas–Israel GPR, Oct. 2023 *Geopolitical*	φ^{dir}	0.0710	***	0.0722	***	0.0448	***
	φ^{GFC}	0.0323	**	0.0003	–	0.0263	+
	φ^{UNC}	-0.0164	***	0.0060	–	0.0014	–
	φ^{LOC}	-0.0275	+	-0.0179	–	-0.0258	+
U.S. Election EPU, Nov. 2024 *Geoeconomic*	φ^{dir}	0.0073	***	0.0132	***	0.0084	***
	φ^{GFC}	-0.0351	***	-0.0463	***	-0.0331	***
	φ^{UNC}	0.0180	***	0.0214	***	0.0316	***
	φ^{LOC}	0.0174	***	0.0151	***	0.0337	***
"Liberation Day" TPU, Apr. 2025 *Geoeconomic*	φ^{dir}	-0.0300	***	-0.0090	***	–	–
	φ^{GFC}	-0.1386	***	-0.0194	*	–	–
	φ^{UNC}	-0.0206	***	0.0264	***	–	–
	φ^{LOC}	-0.0529	***	0.0319	**	–	–

Notes: Estimated impulse responses from narrative local projections using dated event dummies within a ± 3-day window around each crisis episode. Standard errors are clustered by country; country fixed effects are included. Contemporaneous controls: global VIX (moving average) and sovereign yield spread (moving average).
$^{***}p < 0.01$, $^{**}p < 0.05$, $^{*}p < 0.10$, $^{+}p < 0.32$ (68% CI); $--$ = not significant at the 10% level.

F.1 Placebo Falsification: Channel-Level Evidence

Figures 14–17 present the channel-level placebo tests for all four episodes, using the driver-specific Shapley–Taylor decomposition (GPR for geopolitical events; EPU and TPU for geoeconomic events). Each panel plots a single channel's cross-country mean response against the placebo envelope constructed from 100 randomly drawn non-event dates.

Figure 14: **Placebo Test (GPR): Russia–Ukraine, Feb. 24, 2022**

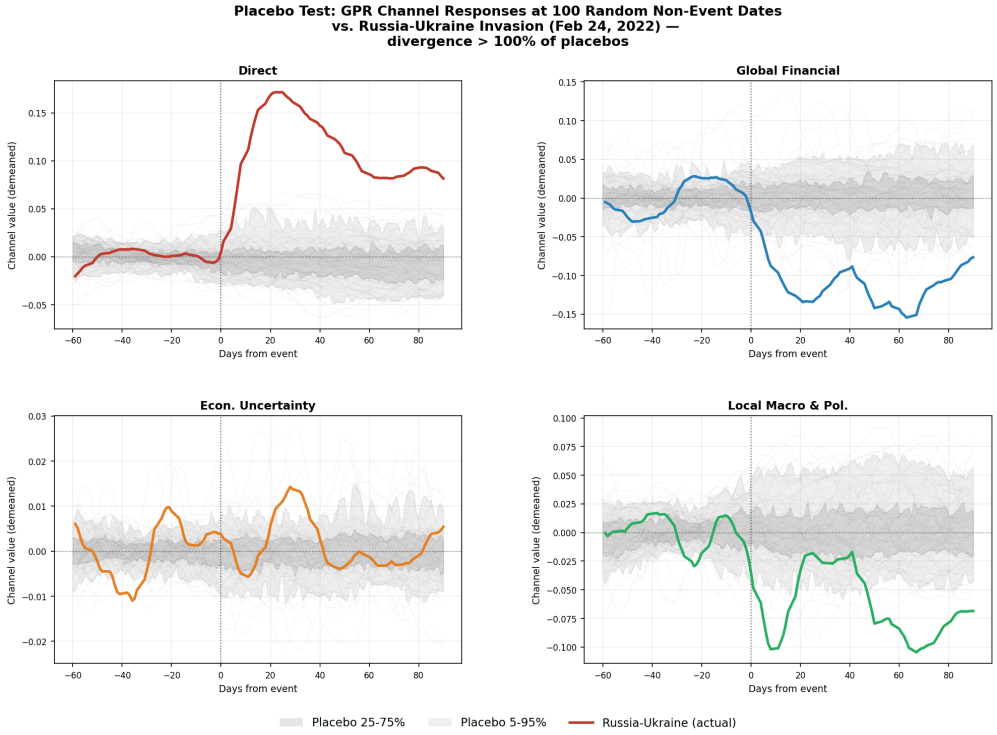

Notes: Channel-level cross-country mean responses vs. 25–75% (dark) and 5–95% (light) placebo bands from 100 random non-event dates. The Direct channel exits the 95th percentile band upward; the GFC channel remains within the placebo range, consistent with geopolitical—rather than geoeconomic—transmission. 7-day trailing MA; values demeaned over the pre-event window.

Figure 15: **Placebo Test (GPR): Hamas–Israel, Oct. 7, 2023 — Divergence > 86% of Placebos**

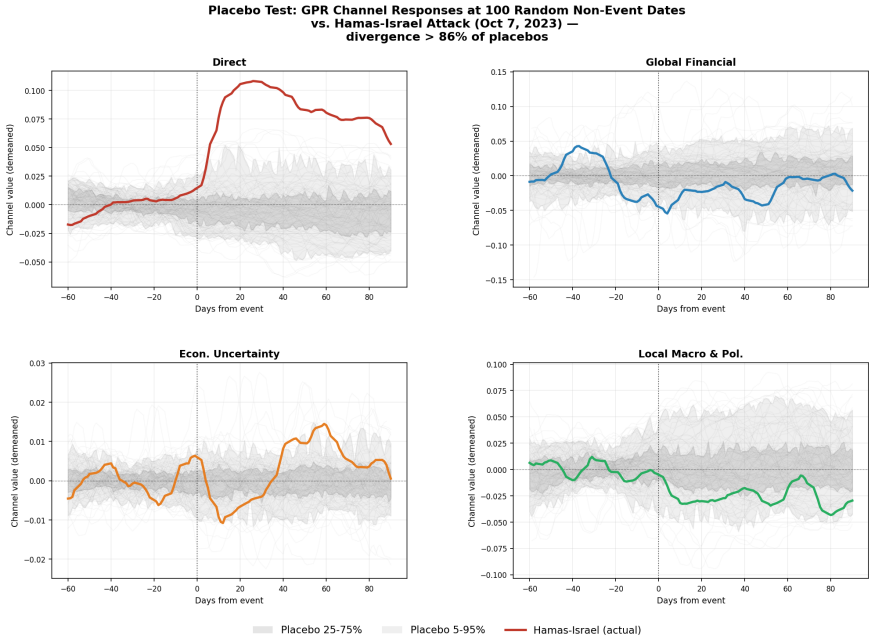

Notes: The Direct channel exits the 95th percentile band upward immediately after day 0, replicating the geopolitical signature observed for Russia–Ukraine. The GFC channel remains largely within the placebo range, consistent with the more regionally contained nature of this conflict. The Uncertainty and Local channels stay inside the bands. 25–75% (dark) and 5–95% (light) placebo bands from 100 random non-event dates. 7-day trailing MA; values demeaned over the pre-event window.

Figure 16: **Placebo Test (EPU): U.S. Presidential Election, Nov. 5, 2024 — Divergence > 83% of Placebos**

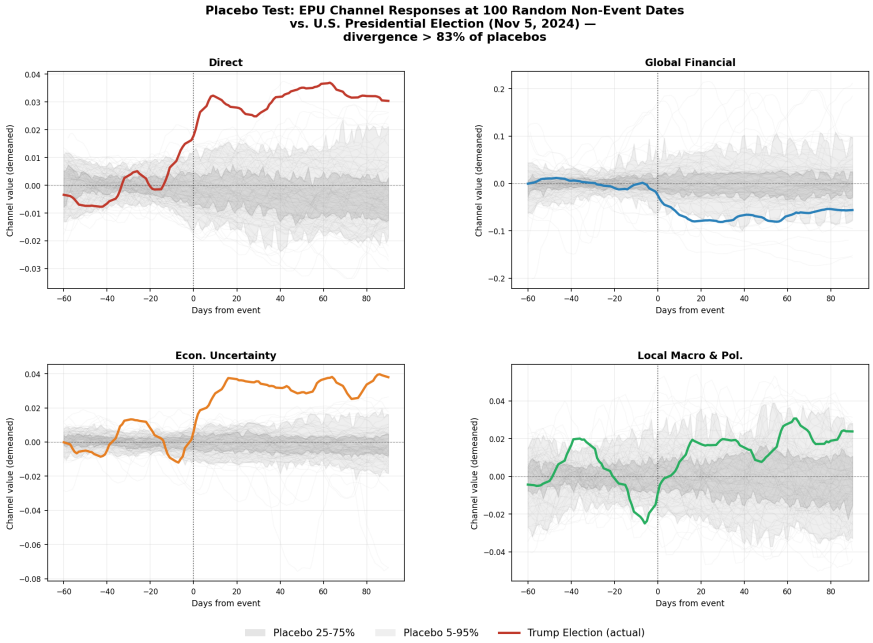

Notes: The Uncertainty channel exits the envelope upward after day 0, consistent with EPU-driven repricing. The GFC channel drops below the band. The Direct channel rises modestly above the envelope, reflecting tariff-related repricing accompanying the election. 25–75% (dark) and 5–95% (light) placebo bands from 100 random non-event dates. 7-day trailing MA; values demeaned over the pre-event window.

Figure 17: **Placebo Test (TPU): Liberation Day Tariff Shock, Apr. 2, 2025 — Divergence > 99% of Placebos**

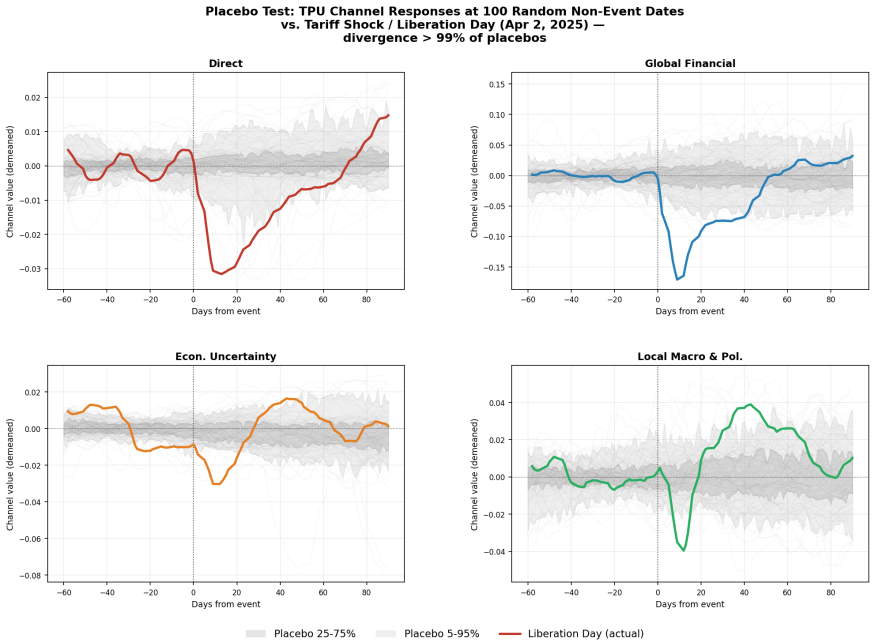

Notes: The GFC channel collapses below the envelope immediately after day 0—the largest single-channel departure across all four episodes. The Direct channel moves *negative*, consistent with the taxonomy's prediction that tariff shocks bypass conflict-proximity repricing. The Local channel exits upward, reflecting heterogeneous tariff exposure. 25–75% (dark) and 5–95% (light) placebo bands from 100 random non-event dates. 7-day trailing MA; values demeaned over the pre-event window.

F.2 Block Bootstrap Validation of Channel Decomposition

Figure 18: **Block Bootstrap Validation of Innovation LP Impulse Responses**

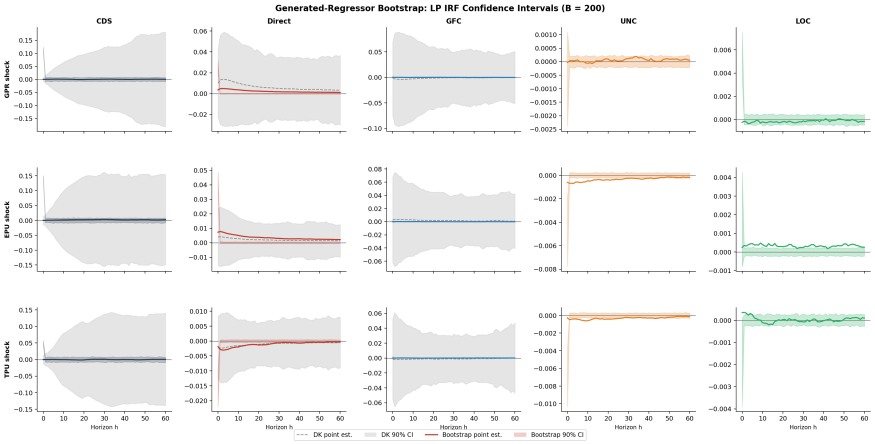

Notes: Each panel plots the innovation LP impulse-response function of a one-standard-deviation shock in the row indicator (GPR, EPU, TPU) on the column variable: the raw CDS spread and the four Shapley–Taylor transmission channels (φ^{DIR}, φ^{GFC}, φ^{UNC}, φ^{LOC}) over horizons $h = 0, \ldots, 65$ days. Dashed grey lines: Driscoll–Kraay (DK) point estimates from the baseline specification (Table 4). Grey shaded bands: DK 90% confidence intervals. Solid coloured lines: median point estimates across $B = 200$ block-bootstrap replications that jointly re-estimate the gradient-boosted tree, recompute the Shapley–Taylor decomposition via TREESHAP, and re-run the panel local projection. Coloured shaded bands: bootstrap 90% confidence intervals (5th–95th percentiles of the replicated IRF distribution). Bootstrap standard errors are uniformly smaller than DK standard errors for $h \geq 7$ (median SE ratio ≈ 0.05 at $h = 30$), confirming that the channel decomposition is stable across re-estimations and that baseline DK inference is conservative.